# Electrosynthesis of Lithium Borohydride from Trimethyl Borate and Hydrogen Gas

By

James Mokaya Omweri

Submitted in Partial Fulfillment of the Requirements

For the Degree of

Master of Science

In the

Chemistry

Program

YOUNGSTOWN STATE UNIVERSITY

December, 2019

**Electrosynthesis of Lithium Borohydride from Trimethyl Borate and Hydrogen Gas**

James Mokaya Omweri

I hereby release this thesis to the public. I understand that this thesis will be made available from the OhioLINK ETD Center and the Maag Library Circulation Desk for public access. I also authorize the University or other individuals to make copies of this thesis as needed for scholarly research.

Signature:

*James Mokaya Omweri*, Student Date

Approvals:

*Dr. Clovis A. Linkous*, Thesis Advisor Date

*Dr. Sherri Lovelace-Cameron*, Committee Member Date

*Dr. Timothy Wagner*, Committee Member Date

*Dr. Salvatore A. Sanders*, Dean of Graduate Studies Date

**ABSTRACT**

Solid state hydrogen storage is seen as the ultimate answer in realizing the hydrogen economy and minimizing our overdependence on nonrenewable fossil fuels. The use of fossil fuels has contributed negatively towards climate change, leading to a lot of future uncertainties. Alkali metal borohydrides, especially lithium borohydride, with desirable $H_2$ storage properties such dry air stability and high gravimetric and volumetric storage densities of 18.5 wt% and 121 kg/m$^3$, respectively, are proving to be some of the most important solid state hydrogen storage materials. However, their current cost of production is very high considering that most borohydrides are synthesized from sodium borohydride, which in turn is made from sodium hydride, NaH, and trimethyl borate, $B(OCH_3)_3$. NaH, which is a product of an energetic process, namely hydrogenation following electrodeposition of the metal from a molten salt, acts as the source of $H^-$ required for the formation of the borohydride ion. In this work, electrochemical transfer of $H^-$ from a Pd foil, which is considered less energetic than NaH, was investigated. Hydrogen gas at a pressure of about 1 atm was passed through the Pd foil, which was used as the working electrode in an electrochemical cell containing 0.1 M $LiClO_4$ and 4.4 M $B(OCH_3)_3$ in $CH_3CN$ as the electrolyte. Using a potentiostat, a voltammetric experiment with 3 cycles at 50 mV/s was performed with and without hydrogen application. A potentiostatic experiment was conducted by holding the Pd foil at -2.75 V vs $Ag/AgClO_4$ and run for 10.6 hours. Analysis of a portion of the electrolyte using IR and NMR spectrometry showed the presence of borohydride. A two compartment cell with Nafion as the separator of the electrode reagents was used to increase the yield.

**ACKNOWLEDGEMENT**

In a very special way, I would like to acknowledge my supervisor, Dr. Clovis A. Linkous for: accepting me to work and deliver this thesis in his research lab, supervising my work, his availability, patience, motivation, experience and immense knowledge on this area and all the thesis writing skills that he imparted on me. Dr. Linkous's chronological order of knowledge presentation from simple to complex was very educative, thank you. Many thanks to Dr. Lovelace Cameron for her time, guidance and every time assurance that all will be well. Thank you for taking your time reading through the draft document and proposing the right corrections. Special thanks to Dr. Timothy Wagner for having time to go through my thesis draft and all the positive criticism on this research. I also thank Mr. Ray for helping in instrumentation.

I would like to expand my sincere thanks to my lab colleagues: Jebet, Patrick, Milica, Kim, Linda and Solita for all the meaningful discussions.

Last but not least, I would like to thank and appreciate my parents, family and close friends for their encouragement. Thank you all.

**Table of Contents**

**List of Figures**

**List of tables**

## Chapter 1: Background Information

### 1.1 Introduction

Energy is the ability to do work; it can either be renewable or non-renewable. Renewable energy sources can be replenished or regenerated. For example:

- Solar energy
- Wind energy
- Biomass
- Ocean current
- Tidal

Other environmentally friendly sources that are not really renewable but provide a huge potential supply are: geothermal, hydroelectricity and nuclear energy. Non-renewable energy sources once depleted cannot be replenished and they are mainly fossil-based e.g:

- Coal
- Petroleum
- Natural gas

The developed world is doing well economically because it has in place many forms of energy. Global energy consumption is on the rise due to increase in population.

The rate at which the world population is increasing, while at the same time available resources such as energy are undergoing depletion, is a worry some trend [1].

The main sources of energy so far are fossil fuels. Figure 1 below by Ridley is a clear indication of how the world depends mainly on fossil fuel sources both for technology, industry and transportation [1].

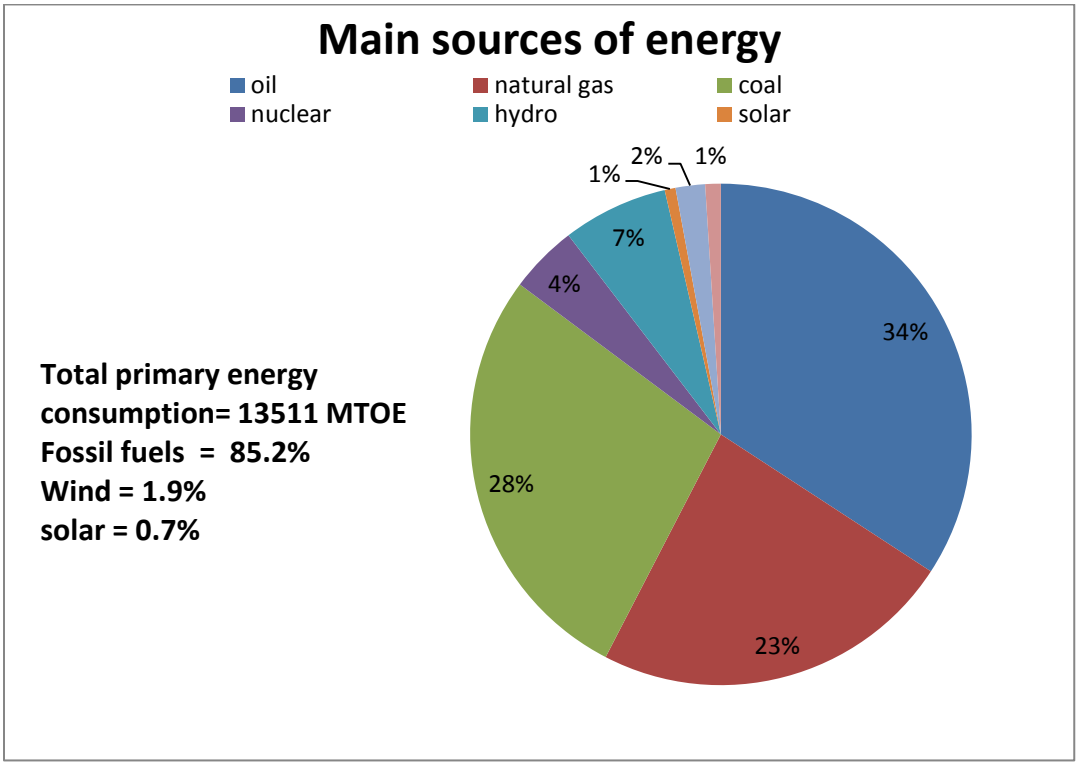


**Figure 1:** World primary energy consumption [1].

Even though fossil fuels are the main source of energy, especially in the transportation sector, its effects are increasingly becoming a concern. Below is a list of some of the main challenges of using fossil fuels:

- Fossil fuel reserves are undergoing depletion
- Oil deposits are unevenly distributed globally; in some areas the ownership of the fuel reserves has become a bone of contention and has led to bloodshed. This is a great challenge for supply and transportation of this commodity.

- The products of burning fossil fuels, such as carbon dioxide and methane (greenhouse gases) are serious contributors to global warming, pollution and other health problems.

This has led to climate change causing environmental degradation. Ridley argues that the world's dependency on fossil fuels, which is estimated to provide 85% of the primary energy source to a population of about 7.5 billion and rising, will lead to climate change due to global warming. Ridley is worried about the slow pace at which alternative energy forms that are cheap, efficient, emission free and abundant are being discovered. Renewable energy sources are a good solution according to Ridley. He notes that with the right research and development (R&D), realistic technological solutions to the harnessing, storage and transportation of alternative renewable energy sources can be achieved [1]. Extensive research on various renewable energy resources is continuing despite challenges in their technology, round trip storage efficiency and application in the transportation sector. To match economic growth, especially for the developed world, and at the same time keep greenhouse gas emissions at a manageable level, an alternative, clean burning, plentiful and sustainable energy source must be developed. This will reduce the overall dependency on fossil fuels. Because of its properties, hydrogen gas has been considered to be the most promising candidate for a clean energy source. This article describes the possibility of hydrogen gas fueling future automobiles [1].

### 1.2 Hydrogen gas as a green energy carrier.

Hydrogen gas qualifies to be a renewable energy carrier if its production relies solely on other renewable sources such as solar energy to split water. This will greatly reduce the greenhouse effect. It has been the chosen candidate for greener energy sources, according to Nagpal and Kakkar [2].

In this thesis, desirable properties of hydrogen are discussed, including:

- Pollution-free source of energy whose main product is water, hence environmentally friendly (no greenhouse gas emissions)
- It is abundant mainly in the form of water, which is everywhere and anybody can access it globally [2].
- Non- toxic
- It has high gravimetric energy density which is approximated to be three times that of gasoline and seven times that generated from coal, according to Lim et al. [3].

Yacobucci and Curtright report the specific density of hydrogen to be 142 MJ/kg, making it an ideal candidate to replace fossil fuels in automobile applications [4].

- Hydrogen can be thermally or electrochemically oxidized in devices such as fuel cells. It provides a rapid half-cell reaction at the anode, releasing energy electrochemically [5]. Fuel cells are just like the internal combustion engine, converting the chemical energy of a fuel into electrical energy.

Figure 2 is a comparison of the gravimetric and volumetric energy densities of various fuels against hydrogen taken from Todorovic [6].

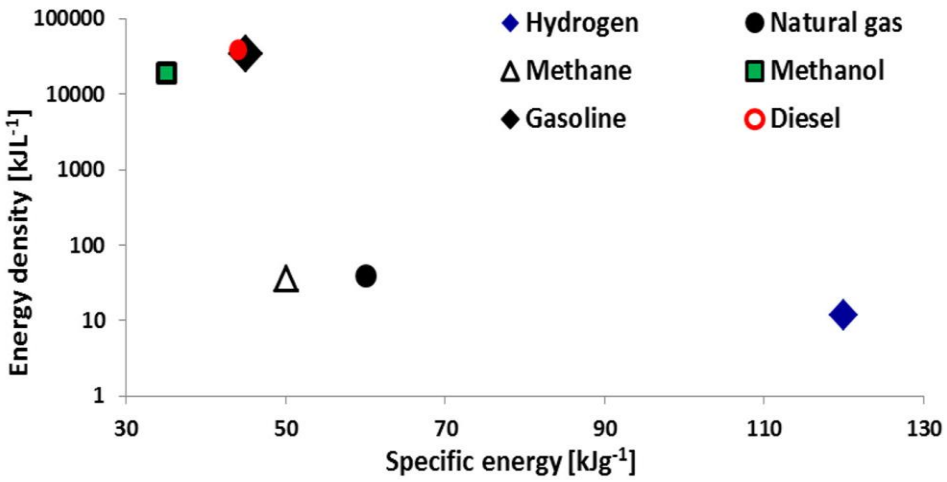


**Figure 2:** Comparison of gravimetric and volumetric energy densities of selected fuels [6].

Thomas and Zalbowitz describe a fuel cell as a device that uses electrochemistry for energy conversion. It takes in fuel such as hydrogen and oxygen and produces electricity, heat and water [7]. The industrial applications of energy from fuel cells have increased overtime, ranging from micro, auxiliary, stationary, portable and military projects to the vehicle industry [8].

Since the introduction of the PEMFC (proton exchange membrane fuel cell), which uses hydrogen as a fuel and gives water as the reaction product, research on the use of hydrogen gas as an onboard fuel in the vehicle industry has intensified. In the PEMFC, $H_2$ as the fuel is separated into protons and electrons at the anode in the presence of a catalyst such as platinum. The protons move through the membrane electrolyte into the cathode where still more platinum catalyst facilitates a reaction between the hydrogen

ions and oxygen gas resulting in the formation of water, while electrons flow through the connecting wire generating a cell voltage. Figure 3 is a schematic diagram of a proton exchange membrane fuel cell.

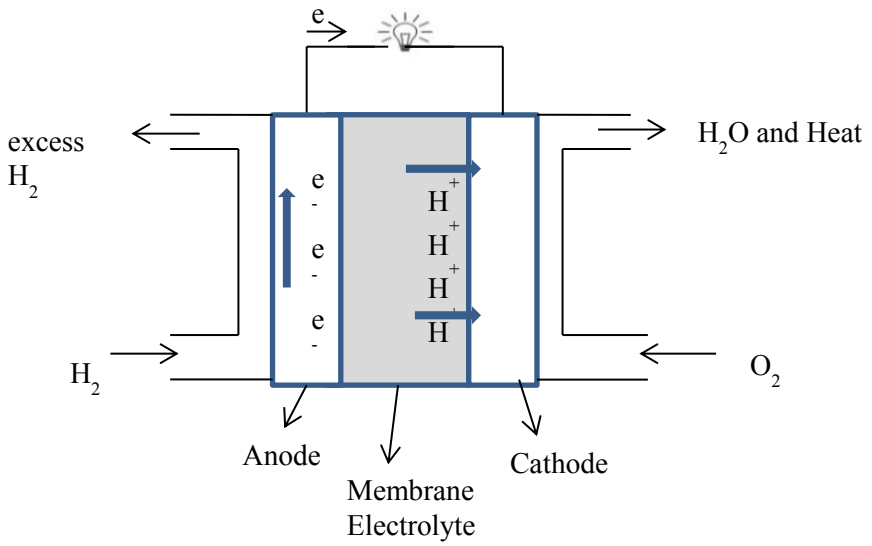


**Figure 3:** Proton Exchange Membrane fuel cell

The membrane is usually made of Nafion$^{TM}$ which is perfluoroether-sulfonated tetrafluoroethylene polymer with desirable thermal and mechanical properties. It also possesses ionic properties, high chemical stability, high water uptake, selective movement of cationic species and does not allow intermixing of oxygen and hydrogen. Finally, it has a high chemical and mechanical resistance [9]. The overall reactions taking place in the PEMFC are described by equations 1 and 2:

$$H_2 \rightarrow 2H^+ + 2e^- \quad (1)$$

$$½O_2 + 2H^+ + 2e^- \rightarrow H_2O \quad (2)$$

R&D on the best utilization of hydrogen in fuel cells is ongoing until that time when it can replace the internal combustion engine and ultimately fossil fuels.

Figure 4 taken from Todorovic [6] paints a picture of a future setup for fuel cell automobiles.

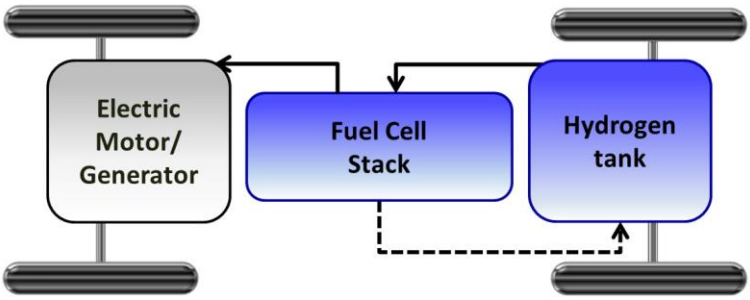


**Figure 4:** Setup for a fuel cell vehicle

However, there are certain properties of hydrogen gas that present a challenge in using it as a fuel:

- Does not exist in free state as a diatomic gas
- "Leaky" due to its high effusion rate associated with its molecular size.
- Highly flammable
- Low liquefaction temperature of 21 K

For the world to transform towards the dream of a hydrogen economy, the cost of production of hydrogen gas from its combined forms, safety issues and storage must be addressed [2].

Todorovic believes in an environmentally acceptable, scientifically possible and technologically viable hydrogen economy. Figure 5 shows a cyclic intent of $H_2$ production taken from Todorovic [6].

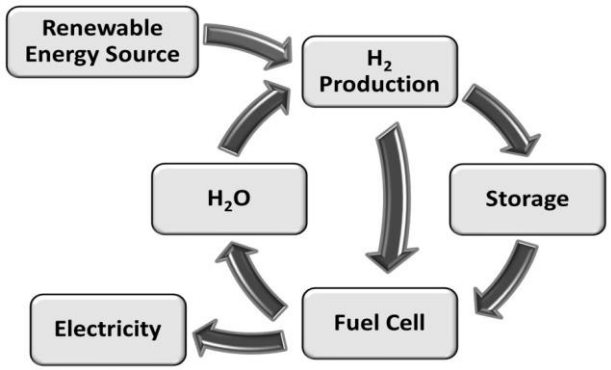


**Figure 5:** The hydrogen fuel cycle [6].

R & D has been carried out on many hydrogen storage materials and it is still going on with an aim of discovering or designing a material which can fulfill the expectations of the hydrogen economy and thus reduce the effects caused by the overdependence on fossil fuels which have really contributed to environmental degradation. Ideally, for a particular material to qualify as a suitable one for hydrogen storage, it must possess some of the following properties:

- High gravimetric and volumetric hydrogen storage capacities
- Absorb and release hydrogen gas rapidly
- Cost-effective and easily available [2].

The US Department of Energy (DOE) sets technical targets in terms of wt% of hydrogen gas in the storage material. For example, for 2017 the set targets were put at 5.5 wt% representing the weight of hydrogen in the material [2].

According to Lim et al., DOE looks at among other attributes:

- Weight and volume of the material
- Cost of production
- Storage lifetime
- Capacity and material reversibility
- Chemistry of absorption and desorption of hydrogen from the material.
- For on-board applications, the refueling time [3].

### 1.3 Hydrogen storage technologies

Generally speaking, many storage methods for stationary and onboard hydrogen have been investigated and the R&D is still going on. Classification of hydrogen storage methods is based on many factors, from gaseous state to liquid state to the solid state. A lot of investigation has been done on these methods, where researchers have delineated both the merits and the drawbacks of each method.

Figure 6 adapted from reference 11 gives a summary of hydrogen storage methods that have been considered so far.

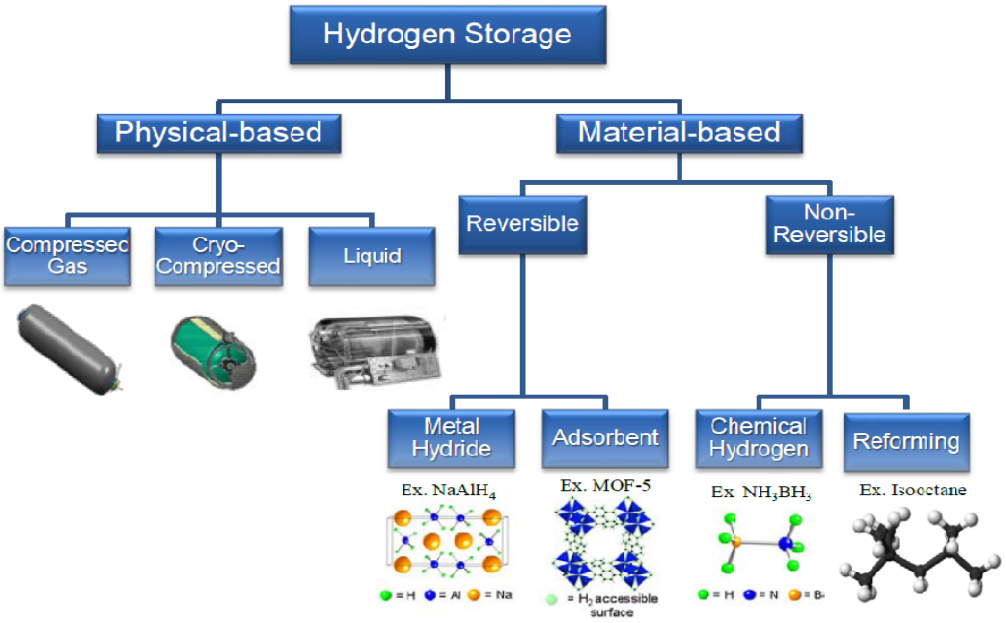


**Figure 6:** Hydrogen storage methods [11].

The ongoing research is now mostly on improvement of the earlier methods in areas such as capacity of storage, cost-effective means of production of hydrogen to compete favorably with other energy sources and safety issues. Understanding the physical properties of hydrogen gas is key in designing a good storage material. Prachi, et al., report some of the storage properties of hydrogen gas, such as density in gas phase as 0.0899 kg/m$^3$ at room temperature, density in liquid phase as 70.8 kg/m$^3$ and boiling point of 20.3 K at atmospheric pressure [10]. Depending on temperature and the pressure, hydrogen gas can be found in various forms.

Figure 7 is a simplified phase diagram for hydrogen as described by Züttel [12].

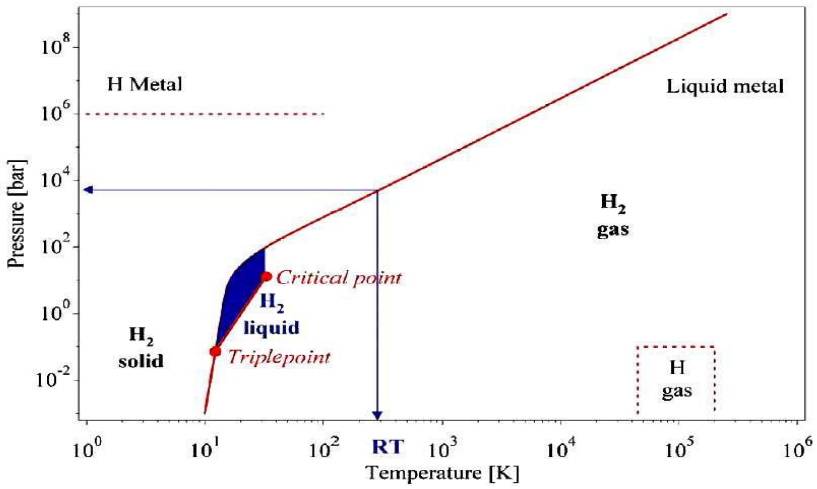


**Figure 7:** Hydrogen phase diagram [12].

Hydrogen storage remains an important challenge for the commercialization of the "hydrogen economy" in automobiles, and stationary and portable applications. Two technical challenges that must be addressed for efficient hydrogen storage are: increase of hydrogen density; and reversibility of hydrogen uptake and release for the method in question. Until a method that meets the weight and volume, durability, refueling time, cost, and safety and performance standards of hydrogen as compared to other fuels is found, hydrogen storage will continue to be a technological barrier to the hydrogen economy. Below is a detailed description of different methods that have been tried and their shortcomings.

## 1.4 Hydrogen storage methods

### High pressure gas cylinders

Different reports have concluded that pressurized gas storage proves to be one of the most reliable technologies for storage of pure hydrogen. There are no additional devices such as reformers, catalysts or coolants required for rapid compression in this hydrogen gas technology. According to Züttel, the cylinders are usually operated at 70 MPa [12]. Container materials with high tensile strength, low density and chemical stability are preferred in this technology. The thickness of the walls of the cylinders is also a factor of consideration, since this increases the mass and decreases the internal volume of the cylinder and thus jeopardizes the gravimetric and volumetric densities [12]. The ideal materials proposed by Todorovic include austenitic stainless steel, or copper or aluminum alloy [6]. In this technology, work is done in compressing the gas first to a given pressure isothermally. Cylinders made of high tensile strength materials can withstand high pressures and this results in high volumetric density, but the problem is a corresponding decrease in the gravimetric density [6, 12]. Züttel reported that the industry set targets at "110 kg, 70 MPa cylinders with 6 wt% gravimetric storage density and 30 $kg \cdot m^{-3}$ volumetric density". To achieve this, a high tensile strength material and a more moderate cylinder pressure should be realized. Even though it is a fairly uncomplicated process, because filling of the tank can take a very short time period, it is evident that the important drawbacks of this method include safety concerns of pressurized gas cylinders, which can autoignite at room temperatures, low density of $H_2$ and energy in acquiring the high hydrogen pressure required. Despite that, this technology seems worthy in stationary applications as opposed to mobile applications.

**Liquid state hydrogen storage**

It is a physical method of hydrogen storage in which cryogenic hydrogen is stored in specialized tanks at -253$^{o}$C and standard pressure. Ross reported a demonstration of the application of liquid hydrogen on automobiles by BMW in which liquid hydrogen is fed into an ICE (internal combustion engine) fitted with a fuel cell. However, hydrogen has to undergo liquefaction, which is achieved through rapid compressions and expansions which require substantial amounts of energy [13]. Züttel quote the theoretical energy required to convert hydrogen gas to liquid at 3.23 kWh·kg$^{-1}$ while the technical one is 15.2 kWh·kg$^{-1}$. This is a substantial fraction of the lower heating value (LHV) of hydrogen [6]. The major drawbacks of this technology include:

- Large amount of energy is required to liquify hydrogen
- The boil-off rate of hydrogen is high due to heat leaks from the storage tanks. Züttel found out that the evaporation rate depends on "size, shape and thermal insulation of the storage vessel" [6].

Lim, et al. concluded that the conventional storage methods of hydrogen gas in high pressure cylindrical tanks and as a liquid in cryogenic tanks are not practical as far as mobile applications are concerned [3].

Basically, these technologies require large amounts of space, as shown by the picture in Figure 8, taken from Schlapbach and Züttel [5].

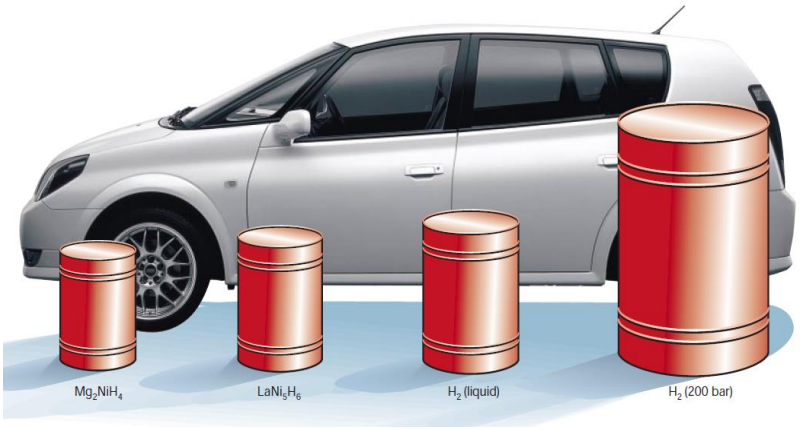


**Figure 8:** Volumetric representation of equal masses of hydrogen gas stored via different methods [5].

The only remaining solution is to explore the solid-state hydrogen storage pathways, which includes physical adsorption methods and chemical compounds. In this category, hydrogen gas is either adsorbed or chemically bonded to the material and can be released on demand. The physical, chemical, reversibility, capacity, production cost, safety and thermodynamic properties of the materials must be taken into consideration.

**Solid state hydrogen storage methods**

In previous sections, the characteristics of gaseous and liquid storage methods have already been described. Even though the storage of hydrogen in the form of high-pressure gas or liquid is possible, safety and security issues, especially in the case of automobile applications, and the enormous amount of energy required for liquefaction or to compress the hydrogen, are important drawbacks.

Solid state hydrogen storage methods have been preferred because of their safety and volumetric and gravimetric capacities. Here the hydrogen either attaches itself to the material surface or reacts chemically with the solid, forming a chemical compound [10]. Lim, et al. pointed out advantage of physisorption methods as having a high efficiency, in that there is reversibility in uptake and release of the hydrogen gas cycles which tends to cast doubt on the reversibility of chemisorption methods. The journal article indicates that during chemisorption, large amounts of the gas are absorbed, but very high temperatures are needed to release the gas from the material. Generally speaking, a good solid-state hydrogen storage material is one that easily absorbs and releases the gas on demand without requiring high temperatures. A reversible hydrogen storage material will be self-sustaining, and this is what researchers want to achieve. "Metal hydrides, metal organic frameworks, zeolites, carbon materials, imides and nitrides" are among the studied methods as reported by Lim, et al. [3]. Schlapbach and Züttel gives a summary of hydrogen gas stored per mass and per volume in solid state storage materials in Figure 9 [5].

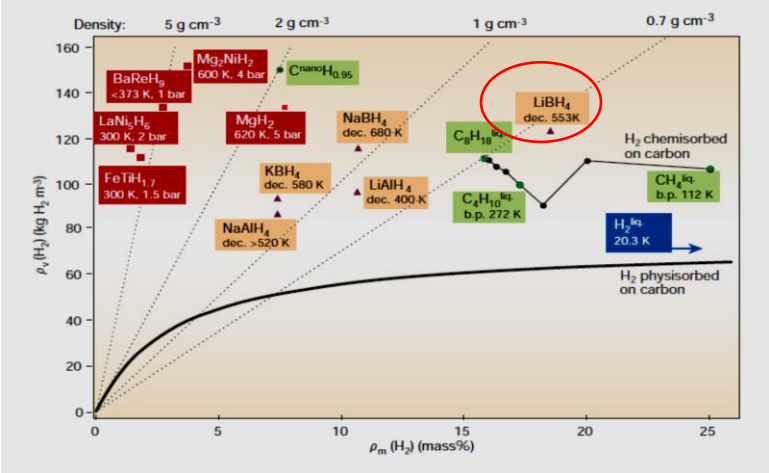


**Figure 9:** Stored hydrogen gas in different materials [5].

**Carbon-based materials through physisorption**

Carbon-based materials have also been proposed for hydrogen storage through the process of physisorption. Carbon is a very common element, which has been used in gas adsorption, purification and removal of poisonous impurities from gases. This is possible because carbon has large surface area, including a porous surface with large pore volume and is chemically stable. Carbon in various forms such as activated carbon, activated carbon fibers and graphite nanofibers have proved to be good adsorbent materials, as reported by Vasiliev et al. [14]. In this technology, $H_2$ weakly interacts with the carbon atoms at the surface where this interaction has been reported to depend on temperature, pressure and nature of the surface of the material. During the interaction process, both attraction and repulsion forces oppose one another, resulting in weak interactions between the hydrogen gas molecules and the adsorbent material. Low temperatures improve this binding process and also doping the surface of the adsorbent material with catalytic nanoparticles such as those of platinum. Dillon et al. have reported a $H_2$ desorption experiment where they quote the gravimetric hydrogen density of 5-10 wt% storage capacity of carbon nanotubes [15].

Whereas in physisorption only adsorption of hydrogen is observed, in chemisorption covalent bonds are involved, where the gas molecules are bonded covalently to the carbon atoms as shown in Figure 10 below adapted from reference 12.

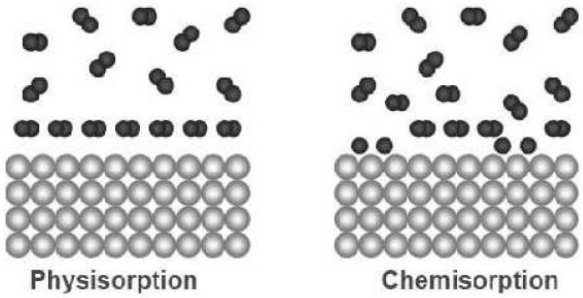


**Figure 10:** Schematic diagrams for chemisorption and physisorption [12].

Reproducibility of the results as far as storage on carbon nanotubes and other carbon based materials has been a challenge and this has been attributed to indeterminate experimental errors and lack of proper characterization of the already developed materials for a follow-up. Tzimas et al. argued that one of the major challenges of this technology is lack of clear understanding of the actual mechanism that surrounds adsorption, desorption and the corresponding capacity of the materials involved [16]. Unlike liquefaction and compressed technologies where high pressures are necessary, this method requires low pressure, cheap materials and non-complicated design systems, however the main challenges are small storage capacity and the low temperatures needed [12].

**Hydrides**

Molecular hydrogen undergoes dissociation into individual atoms when it comes into contact with certain solid materials. The atoms then diffuse into the material forming a chemical bond resulting in the formation of hydrides.

This is a type of chemisorption. A hydride therefore is basically a compound formed when a hydrogen atom reacts with a more electropositive element. Some metals and their alloys react with hydrogen forming the corresponding metal hydrides, which have been found to be good hydrogen storage materials. Formation of these hydrides can be achieved through chemical bonding of the hydrogen atoms after dissociation or by splitting water electrochemically as shown by Equations 3 and 4, Where M is a metal and x =1,2,3 [10].

$$M + \frac{X}{2} H_2 \leftrightarrow MH_X \quad (3)$$

$$M + \frac{X}{2} H_2O + \frac{X}{2} e^- \leftrightarrow MH_X + \frac{X}{2} OH^- \quad (4)$$

**Metal hydrides**

They are formed as a result of hydrogen absorption by a metal. The hydrogen atoms get trapped in the interstitial sites of the metals assuming a general formula of $MH_n$, which is limited to only n = 1, 2 and 3 as described by Fernandes [17]. One of the highly researched categories of the hydrides are the metallic hydrides which are good hydrogen storage materials. Züttel describes one of their general formulae as $AB_xH_n$ where A is a rare earth metal and B is a transition metal that forms unstable hydrides.

Figure 11 taken from reference 12 is a graphical representation of the energies involved when hydrogen reacts with a metal to form hydrides. The graph indicates that energy is released during $H_2$ uptake and must be resupplied upon its release.

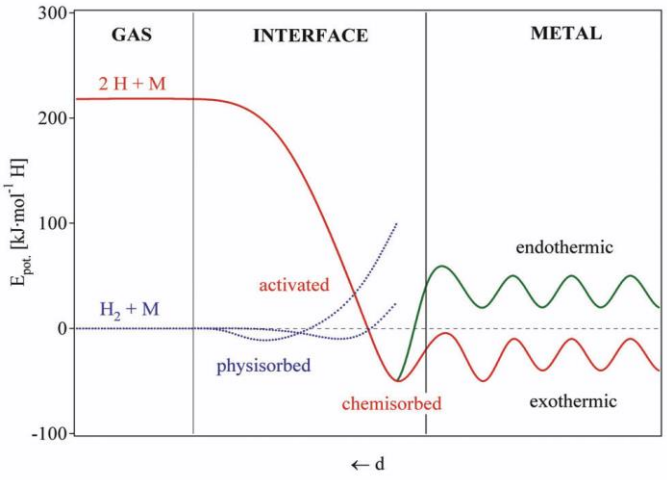


**Figure 11:** Energies involved in chemisorption and physisorption of hydrogen gas onto metal surfaces. [12].

Among the most investigated intermetallic hydrides for hydrogen storage are the $AB_5$, $AB_2$ and AB formulas as reported by Bououdina et al. [18]. $LaNi_5$ is an example of $AB_5$ that has been investigated by several research groups because of its low working pressure and temperature. It also blends well with metals and metal alloys in an effort to improve on the absorption property. Pure $LaNi_5$ has been estimated to absorb about 1.0 H/ $LaNi_5$, which represents roughly 1.5 wt% in gravimetric density. However promising it is, its major drawbacks are high cost, low storage capacity and it is used up quickly within a few cycles. Thus the material falls short of the DOE target of 6.5 wt% as reported by Sakintuna et al. [19]. Sakintuna et al. reported that because of the potential of this $AB_5$ type compound to be used as an on-board hydrogen storage material, researchers have been investigating the effects of milling, mechanical alloying and surface treatment of the

material in order to improve the gravimetric density and the kinetics of the hydriding and dehydriding processes. Derived metal alloys from $LaNi_5$ have shown very promising properties, such as fast and reversible sorption and good cycling life. The volumetric hydrogen density of $LaNi_5H_{6.5}$ at a pressure of 2 bars is equivalent to that of gaseous molecular hydrogen at a pressure of 1,800 bars, but the main advantage is that all the hydrogen is desorbed at a pressure of 2 bars. Since lanthanum and nickel are heavy elements, the density of hydrogen in $LaNi_5H_{6.5}$ remains below 2 wt%, but is still very attractive for electrochemical hydrogen storage in rechargeable metal hydride electrodes, [20, 21].

The $AB_2$ group consists of either Ti or Zr as A and any of the 3d ( Fe ,V, Mn and Cr) elements on the B site. The gravimetric density of these hydrides can go up to 2 wt% as reported by Kuriiwa et al. [22]. Reports indicate that the $AB_2$ hydrides have shown high storage capacities, faster kinetics and have longer cycling life and are relatively cheap. One of their important challenges is their stability at low ambient temperatures, as reported by Bououdina et al. FeTi is an AB type metal hydride whose hydrogen storage properties have been widely studied. Its hydrogen storage capacity has been reported to be 1.90 wt% according to Sakintuna et al. [19]. The capacity was found to improve when elements with catalytic ability such palladium were added to it during activation. An important challenge in improving the storing properties of this hydride is the formation of a layer of titanium oxide, which hinders the activation process. High pressure and temperature requirements are also major drawbacks for this hydride in achieving reasonable and reproducible absorption/desorption amounts of hydrogen gas [20].

The PCT (pressure composition temperature) properties of selected metal hydrides are shown in Figure 12 and adapted from reference 12. The PCT profiles describe the process of absorption and desorption of hydrogen gas by intermetallic hydrides.

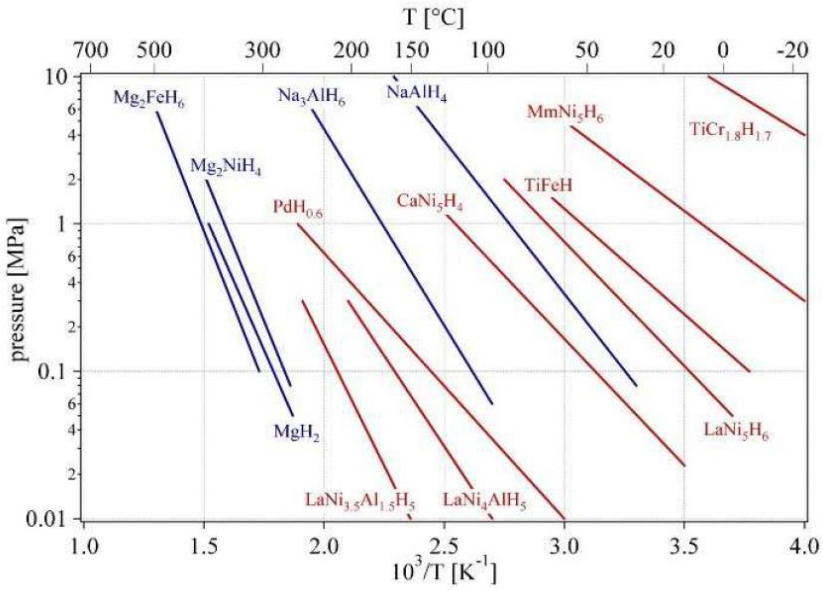


**Figure 12:** Van't Hoff plots of some selected hydrides [12].

Even though promising, metal hydrides have a few drawbacks such as low mass density and heavy containers whose weight must be lowered drastically. Some of the metals used for hydrides are very expensive, for example, Pd. There are less expensive options, but they require extremely high temperatures to release the hydrogen.

**Complex hydrides**

According to Züttel, complex hydrides can either be ionic or covalent and they are formed by the reaction between complexes $BH_4^-$, $AlH_4^-$ or $NH_2^-$ by electropositive metals from groups 1, 2 and 3. These compounds are very stable, but if subjected to high temperatures, they decompose [12]. Because of their light weight and high storage capacities, they have drawn more attention for studies in hydrogen economy [23].

Production cost, kinetics and thermodynamic properties are among the most researched areas on these compounds. Recent work has shown that their potential use as reversible hydrogen storage materials has been realized. This is due to the discovery of the catalytic enhancement by Ti-doping of the hydrogenation/dehydrogenation process [24]. Chemical hydrides can be classified into two groups, namely: binary hydrides and complex hydrides. In simple hydrides, the hydrogen is bonded covalently or ionically to a single metal, while in complex hydrides, the hydrogen is held in the form of a complex anion. A number of different hydrides have been studied for hydrogen storage. Figure 13 shows the gravimetric density of $H_2$ for the most promising chemical hydrides and the maximum amount of hydrogen deliverable via hydrolysis of the respective hydride. The storage capacity of hydrogen gas adsorbed onto a material and or even compressed within the material can be calculated and is usually expressed in units of wt%.

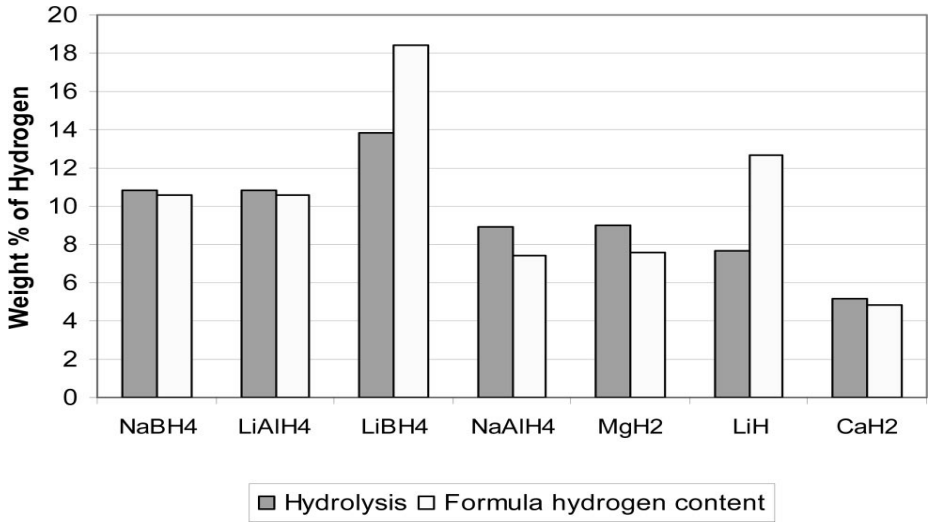


**Figure 13:** Maximum deliverable hydrogen from hydrolysis of ionic hydrides [19].

Chemical hydrides are a promising solution in overcoming the issues related to hydrogen safety and handling and are competitive with respect to conventional fuel.

**Alanates**

These are compounds of Al, an alkali metal and hydrogen. The best example is sodium tetrahydroaluminate, $NaAlH_4$, with a hydrogen storage capacity of 5.6 wt%. It has been found to be a promising candidate for $H_2$ storage for on-board applications because of its low cost and relative abundance according to Sakintuna et al. [19]. Decomposition of this compound is described by equation 5 taken from reference 13.

$$3\ NaAlH_4 \rightarrow Na_3AlH_6 + 2\ Al + 3\ H_2 \rightarrow 3\ NaH + 3\ Al + \frac{9}{2}\ H_2 \qquad (5)$$

The absorption/desorption rates of $H_2$ are found to increase when small quantities of $TiCl_3$ are added for activation as reported by Bogdanovich and Schwickardi [24].

**Imides and amides**

Chen et al. indicated that Li-N-H systems can also be used as $H_2$ storage systems for on-board applications, since the systems can store slightly more than 10 wt% reversibly. Equations 6 and 7 below taken from reference 25 show a two-step hydrogenation and dehydrogenation of an $Li_3N$ system even though only the second step is reversible.

$$Li_3N + \frac{3}{2}H_2 \rightarrow Li_2NH_2 + LiH \qquad (6)$$

$$Li_2NH_2 + \frac{1}{2}H_2 \leftrightarrow NH_2 + 2LiH \qquad (7)$$

The major drawback of this system is the decomposition temperature, which is too high for practical applications [25].

Many related systems have been investigated, including Li-Mg-N-H as far as $H_2$ absorption and desorption properties are concerned and on how they depend on

temperature. The system still experiences poor kinetics even at fairly elevated temperatures as high as 200$^{o}$C as reported by Luo [26].

### 1.5 Borohydrides

The reaction of light metals such as Al, Na, Mg, Li and Be with the complex ion, $BH_4^-$ (borohydride ion) gives rise to one of the most researched lightweight materials for hydrogen storage. These metal hydrogen complexes have been found to have a high density of hydrogen atoms per metal atom. Because of this, they have high volumetric storage capacities. The hydrogen atoms sit at the corners of a tetrahedron with a B atom at the center. The anionic effect of $BH_4^-$ is canceled out by the cationic effect of the metals [27]. Table 1 below taken from Prachi et al. [10] shows some of the properties of complex boron hydrides

**Table 1:** Properties of complex boron hydrides[10].

| | Molecular weight (g/mol) | Melting point ($^0$C) | Start of decomposition ($^0$C) | Hydrogen content (wt%) |
|---|---|---|---|---|
| $LiBH_4$ | 21.8 | 275 | 320 | 18.4 |
| $NaBH_4$ | 37.8 | 505 | 45 | 10.6 |
| $KBH_4$ | 53.9 | 585 | 584 | 7.4 |
| $Be(BH_4)_2$ | 38.6 | -- | -- | 20.7 |
| $Mg(BH_4)_2$ | 53.9 | -- | 320 | 14.8 |
| $Ca(BH_4)_2$ | 69.8 | -- | 360 | 11.5 |
| $Al(BH_4)_3$ | 71.4 | -64 | 40 | 16.8 |

Because of their high gravimetric and volumetric hydrogen storage capacities, borohydrides have been of great interest as far as solid state hydrogen storage is concerned. However, their thermodynamic and kinetic properties present major drawbacks in terms of hydrogen desorption and absorption.

For these materials to be major contributors towards realizing the hydrogen economy, the thermodynamic and kinetic properties must be favorable, and above all, they must show reversibility. R&D is still going on in areas of finding a cost-effective way of producing them and also tailoring efforts to improve their kinetics. Below is a brief description of $NaBH_4$ and $LiBH_4$ as hydrogen storage materials.

**Sodium borohydride, $NaBH_4$**

Sodium borohydride is an important chemical in many industrial processes such as a reducing agent in organic synthesis, water treatment, paper pulp industry and a solid material for hydrogen storage [28]. One major drawback of using sodium borohydride in the hydrogen economy is its high current cost of production and regeneration. This method is based on synthetic routes that were developed more than six decades ago by Brown and Schlesinger as reported by Wu et al. [28]. Since then, many R&D centers have proposed different pathways that can be cost effective. Wu et al. outlined some of the recent methods of sodium borohydride production as follows:

The Brown and Schlesinger process is the established method for $NaBH_4$ production. It begins with the production or acquisition of raw materials first such as sodium metal, hydrogen gas and pure trimethyl borate. Sodium metal reacts with hydrogen to form sodium hydride, which is then reacted with trimethyl borate to form sodium borohydride and sodium methoxide, as per equation 8.

$$4NaH + B(OCH_3)_3 \rightarrow NaBH_4 + 3NaOCH_3 \quad (8)$$

Figure 14 is a schematic diagram taken from reference 28 summarizing the steps in the Brown and Schlesinger process of manufacturing sodium borohydride.

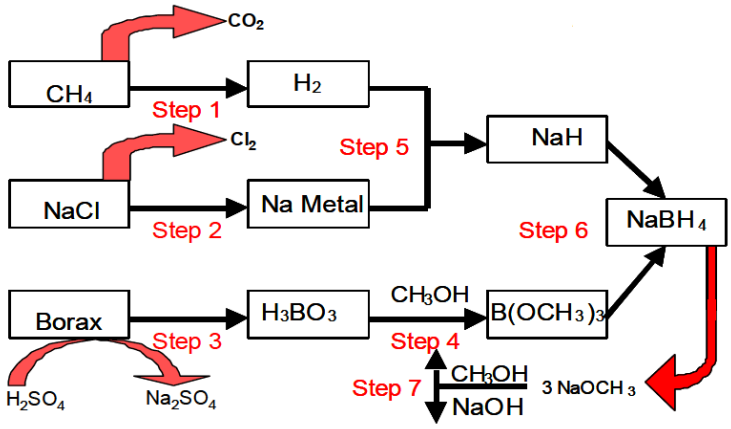


**Figure 14:** Brown and Schlesinger process for synthesis of $NaBH_4$ [28].

The $H^-$ source in this process, NaH, is obtained through a reaction of sodium metal and hydrogen gas. Manufacture of sodium metal is through electrolysis of molten sodium chloride while hydrogen gas is obtained from natural gas. $B(OCH_3)_3$ is produced by first treating borax mineral with sulfuric acid to obtain boric acid, which is finally reacted with methanol. Production of sodium metal through molten electrolysis salt is heavy energy consuming process and thus is a bit costly.

Another highly discussed method is the Bayer process, which is a one pot synthesis where all the required raw materials are put in one reaction vessel at once, equation 9 describes this reaction

$$Na_2B_4O_7 + 16Na + 8H_2 + 7SiO_2 \rightarrow 4NaBH_4 + 7Na_2SiO_3 \quad (9)$$

Being a one pot reaction is very attractive but the cost of sodium metal is still expensive. Secondly, sodium silicate build-up is a challenge considering that its demand is very low and therefore requires well organized disposal means.

**Lithium Borohydride, $LiBH_4$**

Lithium borohydride is also a strong reducing agent in organic and inorganic reactions. Because of its high hydrogen storage properties, $LiBH_4$ has attracted many scientists to do research on its storage capacity and how it can be produced in large scale and in a cost-effect manner. Soulie´ et al. report that lithium borohydride has an orthorhombic symmetry with "[space group *Pnma*, $a$ = 57.17858(4), $b$ = 54.43686(2), $c$ = 56.80321(4) $A^o$]", structure [29]. The gravimetric hydrogen density of lithium borohydride has been reported to be 18.5 wt%, while the volumetric density is 121 kg/m$^3$. It has a density of 0.666 g/cm$^3$, a melting point of 275 $^o$C and a boiling point of 380$^o$C [27]. Züttel et al. summarize the values of the thermodynamic functions of the borohydride at 25·15 $^o$C, as follows: $\Delta H_f$ = -194.44 kJ·mol$^{-1}$, $\Delta G$ = -128.96 kJ·mol$^{-1}$, $S^0$ = 75.91 J·K$^{-1}$.mol$^{-1}$, $c_p$ = 82.60 J·K$^{-1}$·mol$^{-1}$ [30]. In terms of stability, it is a very stable compound with a high lattice energy of 779 kJ·mol$^{-1}$. It releases the stored hydrogen through decomposition by heat or reaction with water as shown in Equations 10 and 11 below. The reaction in Equation 10 was described by Ross [13], and the reaction in Equation 11 was described by Ross as well, but in an analogous manner using sodium borohydride.

$$LiBH_4 \rightarrow LiH + B + \frac{3}{2}H_2 \quad (10)$$

$$LiBH_4 + 2H_2O \rightarrow 4H_2 + LiBO_2 \quad (11)$$

Borohydrides have also high gravimetric storage capacities as shown in Table 1. The theoretical gravimetric capacities of $NaBH_4$, $KBH_4$, and $Mg(BH_4)_2$ are 10.5, 7.4 and 14.8 wt% respectively. Borohydrides are moisture sensitive; Eberle et al. [31], note that the possible evolution of volatile boranes, even at small levels, would be problematic due to

storage capacity loss and fuel cell damage. Walker [32] has discussed the destabilization of complex hydrides through mixing with other compounds. For example, he has argued that $LiBH_4$ can be mixed with various additives, including hydrides such as $MgH_2$, magnesium salts ($MgF_2$, $MgS_2$ and $MgSe_2$), elemental metals (Al), alloys, oxides ($TiO_2$) and carbon. This brings about modifications on borohydrides, as well as other complex hydrides, that constitute new promising candidates for hydrogen storage, and are likely to be an interesting area of continued research.

The alkali metal borohydrides are now over 60 years old since their preparation was reported in 1940 by Schlesinger and Brown. In their work, they reacted ethyl lithium as the precursor material with gaseous diborane, and lithium borohydride was formed according to Equation 12.

$$3LiC_2H_5 + 2B_2H_6 \rightarrow 3LiBH_4 + (C_2H_5)_3B \quad (12)$$

They also established that the compound formed had a melting point of between 275-280$^oC$ and that when exposed to the atmosphere, it reacted with moisture but remained stable in dry air [33]. Schlesinger and other US scientists went on with the search on how to prepare larger quantities of alkali metal borohydrides between 1952-1953 using any alternative procedures [34]. These efforts led to another new method of borohydride preparation; a reaction between lithium hydride and diborane in the presence of diethyl ether as a solvent was reported by Schlesinger et al. The reaction occurred as per Equation 13 with evolution of heat [35].

$$2LiH + 2B_2H_6 \rightarrow 2LiBH_4 \cdot Et_2O \quad (13)$$

The solvent was removed by heating the intermediate product to a temperature of 100$^{o}$C in vacuum and pure lithium borohydride was obtained. Contrary to the above claims by Schlesinger et al. that the reaction could only take place in the presence of a solvent, Friedrichs, et al. reported that the reaction can indeed go on without the solvent environment. In their work, they reacted lithium hydride and diborane at 120 $^{o}$C and ambient pressure and a yield of 74% was realized [36]. Perturbed by the quantities of borohydride produced in the lab and safety concerns presented by handling diborane, Schlesinger and company continued with the search of a suitable procedure that could be used in an industrial scale production of alkali metal borohydrides. In one of their attempts to make sodium borohydride, they heated sodium trimethoxyborohydride to temperatures of about 230 $^{o}$C expecting the reaction shown in Equation 14 to take place [34].

$$4NaBH(OCH_3)_3 \rightarrow NaBH_4 + 3\ NaB(OCH_3)_4 \qquad (14)$$

The reaction did not proceed to the end, and in the process of improving the reaction conditions, Schlesinger et al. noted that sodium hydride and trimethyl borate, both intermediate products of reaction 11, reacted to give good yields of sodium borohydride at temperatures of between 225-275 $^{o}$C. This is shown in Equation 15 [34].

$$4NaH + B(OCH_3)_3 \rightarrow NaBH_4 + 3NaOCH_3 \qquad (15)$$

The yield of sodium borohydride was reported to be 96% and its purity was high.

A yield of 70% lithium hydride was realized using the same method by reacting lithium hydride and trimethyl borate as in Equation 16 [34].

$$4LiH + B(OCH_3)_3 \rightarrow LiBH_4 + 3LiOCH_3 \quad (16)$$

Nevertheless, the urge to produce quantifiable amounts of alkali metal borohydrides went on. In 1953, Schlesinger, Brown and Hyde reported a new method of preparation of the borohydrides. They observed that when excess lithium chloride was added to sodium borohydride in isopropylamine, a yield of over 90% lithium borohydride was obtained, as in Equation 17 [37].

$$NaBH_4 + LiCl \rightarrow LiBH_4 + NaCl \quad (17)$$

This is the current method in use to prepare lithium borohydride. It is considered expensive because one of the starting materials, sodium borohydride, is a product of an energetic process which involves obtaining sodium metal through electrolysis before reacting it with hydrogen to form sodium hydride. Sodium hydride is the source of $H^-$, which is accepted by the boron atom due to its Lewis acid properties. Any procedure that will use a different source of $H^-$ for hydriding purposes is believed to lower the cost of production of lithium borohydride, and considering its storage capacity of hydrogen gas, the hydrogen economy can be realized. In this work, electrochemical transfer of the $H^-$ to $B(OCH_3)_3$ in an electrolytic cell over the surface of a palladium foil as the working electrode in a non-aqueous medium is investigated.

## 1.6 Objective

The objective of this work is to use electrochemistry as a means of synthesizing lithium borohydride, $LiBH_4$, through electrochemical hydriding of trimethyl borate, $B(OCH_3)_3$ in a non-aqueous electrolyte contained in a specially constructed electroanalytical cell.

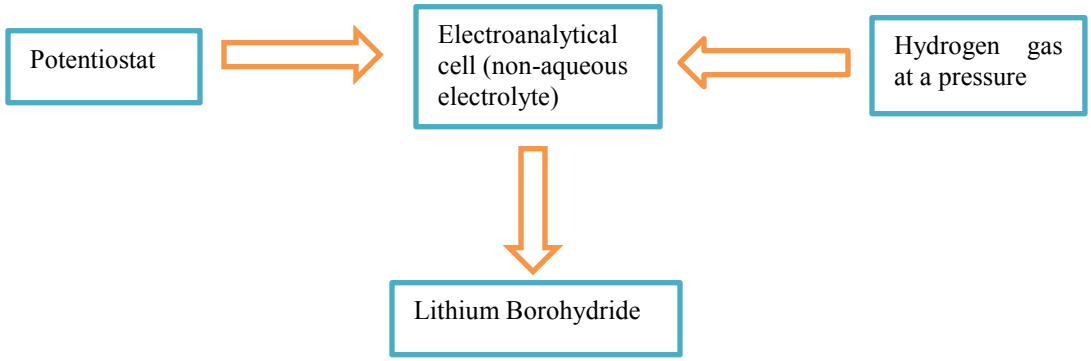


**Figure 15:** Schematic diagram of the proposed study.

## 1.7 Hypothesis

Realization of hydrogen economy has been elusive due to the nature of difficulties in storing hydrogen gas safely and also in a manner that it can be used in mobile applications. Owing to its properties, solid state hydrogen storage especially by chemical hydrides has been promising, considering their light weight and good volumetric and gravimetric storage capacities. One such complex hydride is lithium borohydride with 18.5 wt% storage capacity. The major drawback of this compound is its high current cost of production involving a reaction between sodium borohydride and excess lithium chloride in a suitable solvent as described by equation 17. In this work, it is sought to develop an inexpensive procedure of providing a different source of $H^-$ for hydriding purposes. This is believed to lower the cost of production of lithium borohydride. In this thesis, electrochemical transfer of the $H^-$ to $B(OCH_3)_3$ in an electroanalytical cell over the

surface of a palladium foil as the working electrode will be investigated. Electrochemical transfer of one $H^-$ to $B(OCH_3)_3$ will lead to the formation of lithium trimethoxy borohydride which at raised temperatures of about 230 $^oC$ will disproportionate to form lithium borohydride as described by equation 18, [34].

$$4LiBH(OCH_3)_3 \rightarrow LiBH_4 + 3LiB(OCH_3)_4 \quad (18)$$

**1.8 Significance of the study**

Realization of the hydrogen economy is the dream of many nations. Solid state hydrogen storage, especially use of complex hydrides, is highly desirable. If successful, this study will provide a safe and inexpensive method for manufacture of solid state materials such as $LiBH_4$, which can be considered for automotive application. Safely stored hydrogen gas has many very important applications such as space shuttle and space missions, industrial processes like manufacture of ammonia and metal refining. This research also involves many analytical procedures that will be very useful to an analytical chemistry student.

## Chapter 2: Instrumentation, materials and experimental methods

### 2.1 Electrochemical Methods

#### Potentiostat

The potentiostat is an electronic instrument that controls the potential applied to a working electrode (WE) relative to the reference electrode (RE). The flow of current is measured between WE and CE (counter electrode) and it remains the measured variable. Operational amplifiers are usually used in construction of this instrument. The WE is usually made up of an inert material such as glassy carbon, gold or platinum. It serves as a surface over which the electrochemical reaction of interest takes place. A constant potential is usually applied to this electrode. The RE is used to measure the working electrode potential and it should possess a constant electrochemical potential as long as no current flows through it. The most common examples are saturated calomel electrode and silver/silver chloride. The counter electrode is just a conductor that completes the circuit and it is also made of inert materials like graphite and platinum and it is through this electrode that the current leaves the solution [38]. Figure 16 is a schematic diagram of a potentiostat circuit that is used to carry out electrochemistry experiments.

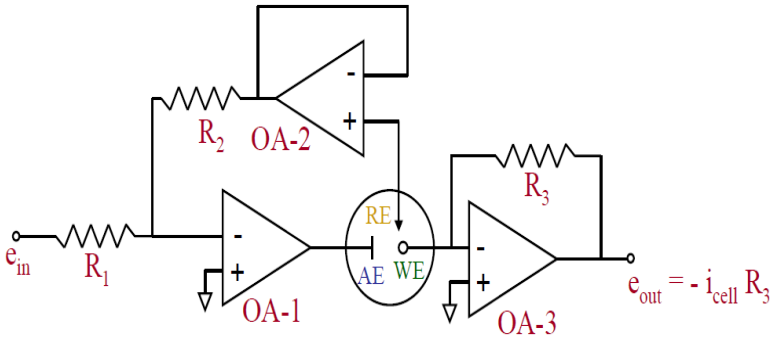


**Figure 16:** A basic potentiostat [38].

**Electrochemistry**

Electrochemistry is a branch of physical chemistry that deals with the study of electricity production by chemical processes through transfer of electrons from one species to another through an external circuit. Mentioning terms like potentiometry and polarography brings out the quantitative aspects of electrochemistry derived directly from the solution thermodynamics. Mechanistic movement of electron transfer processes and their kinetic properties have been a subject of study by different groups. In general, electrochemistry is increasingly being used to probe redox reactions. Sawyer and Roberts noted that new applications of electrochemistry encompass even adsorption phenomena. Heterogeneous electron transfer redox reactions can now be studied through thermodynamic and kinetic measurements.

In the areas of organic and inorganic chemistry, unstable or difficult to obtain species can now be synthesized electrochemically. In the field of analytical chemistry, electrochemical techniques have been used for chemical characterization analogous to other analytical methods such as infrared, ultraviolet-visible, NMR and ESR [39]. In their book, Sawyer and Roberts outlined some of the questions that electrochemistry seek to answer including: "determining the standard electrode potentials for the couple involved in the redox reaction, thermodynamic properties of the solution in question, electron stoichiometry of a redox couple, electron transfer kinetics of a species in the solution under study, determining the effect of the solvent, supporting electrolyte and electrode material on the electrochemical process and finally synthesis and study of unstable intermediates [39]. Strictly speaking, electrochemical techniques are very sensitive; therefore, before any analysis, the researcher must select the proper electrochemical

method and the corresponding sample conditions. Properties of the sample, such as solubility and stability are very important indicators of the type of solvent and the supporting electrolyte that can be used. The chosen solvent must be electrochemically compatible and the supporting electrolyte must dissolve in the solvent without interfering [39]. The most widely applied electrochemical techniques include: potentiometry, coulometry and voltammetry. The literatures show that various electrochemical syntheses have been tried with little success. Most of these cases have been done in aqueous medium. Proposed use of electrochemical techniques in the synthesis of borohydrides for hydrogen storage will greatly reduce the cost of production compared to the existing chemical synthetic processes. Electrochemical reduction of borate salts requires an input of electrical energy and has been considered to be a simpler process unlike other methods discussed earlier.

One of the key challenges in solid state hydrogen storage is the question of recyclability of the process after hydrogen release. Electrosynthesis seems to be the answer to this problem, as reported in many of the patents from 1958 to 1990. Caroline et al. report the regeneration of $NaBH_4$ through use of an electrolytic cell to reduce spent $NaBO_2$. This route is considered efficient in terms of less harmful emissions and also lesser amounts of electrical energy used. The following equations, 19, 20 and 21 describe the direct electroreduction of $NaBO_2$:

$$\text{Cathode: } BO_2^- + 6H_2O + 8e^- \rightarrow BH_4^- + 8OH^- \quad (19)$$

$$\text{Anode: } 8OH^- \rightarrow 4H_2O + 2O_2 + 8e^- \quad (20)$$

$$\text{Overall: } BO_2^- + 2H_2O \rightarrow BH_4^- + 2O_2 \quad (21)$$

No significant amount of borohydride was reported from this procedure, despite claims from a number of patents [40].

Gyenge and Oloman [41], attempted the electroreduction of borate esters using organic solvents and lithium salts as supporting electrolytes. Hexamethylphosphoramide (HMPA)-ethanol mixture and ethylenediamine (EDA) were employed as the catholytes. No detectable amount of the borohydride was reported.

Linkous C.A (2003-4), at the Florida Solar Energy Center, hydrogen R&D division, University of Central Florida, proposed an electrochemical version of the Schlesinger process, in which sodium borohydride is formed by a reaction between adsorbed hydrogen and trimethoxy borate as reported by Caroline et al.

**Cyclic voltammetry**

Cyclic voltammetry is mostly applied to determine the reduction and oxidation processes of species under electrochemical study. In cyclic voltammetry, the potential is scanned in one direction. It can be either to a more positive or more negative potential. If the electrochemistry is carried out in an unstirred solution, then the resulting voltammograms have peak currents instead of limiting currents as shown below in Figure 17 adapted from reference 42.

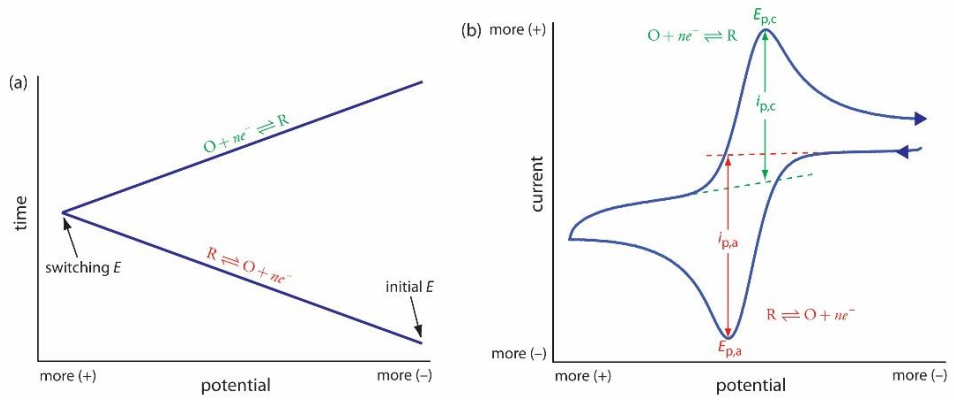


**Figure 17:** Cyclic voltammogram showing oxidation and reduction processes after scan [42].

An electrochemical cell such as one used in Figure 18 is usually used for experimentation in cyclic voltammetry

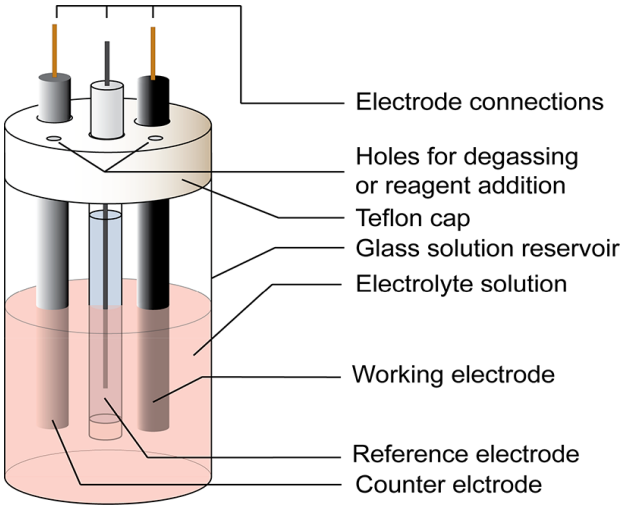


**Figure 18:** An electrochemical cell for cyclic voltammetry [43].

The electrolyte solution containing the solvent and the supporting electrolyte must be well prepared before carrying out a CV experiment. The supporting electrolyte, which is basically a dissolved salt, is used to decrease the resistance of the solution.

According to Elgrishi et al., a good solvent must have the following properties: must be a liquid at the experimental temperatures and should completely dissolve both the analyte and the supporting electrolyte, should not undergo oxidation or reduction within the potential window of the experiment and finally should not react with either the analyte nor the supporting electrolyte. On the other hand, the supporting electrolyte must be highly soluble in the chosen solvent, purifiable and inert both chemically and electrochemically within the potential window [43]. The electrochemical window of the solvent should be carefully determined, because it has been shown that the nature of the electrolyte, type of solvent and the nature of material of the working electrode used all determine the potential window that can be used to undertake a particular CV experiment [44, 45].

Figure 19 is a diagram adapted from reference 43 showing the effects of the mentioned factors on the potential window of different solvents.

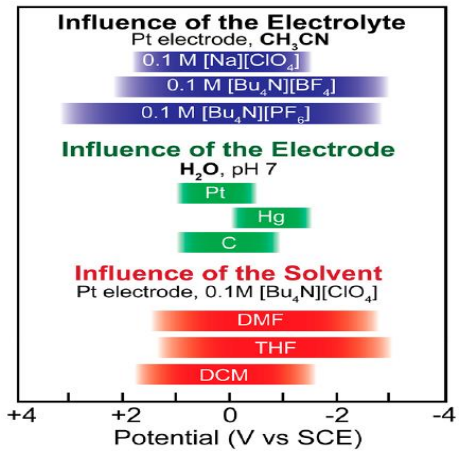


**Figure 19**: Effect on Potential window for different solvents, electrodes and supporting electrolytes [43].

During data acquisition in a CV experiment, the first experiment is done with a blank electrolyte without the analyte to ensure that all the experimental components and connections are in good shape. Even though the electrolyte is blank, a small current due to non-faradaic activity is registered. This is then followed by addition of an analyte that has undergone a spurge to create an inert atmosphere. This keeps away oxygen gas, which is commonly electroactive and may otherwise interfere with the voltammetric curve [43]. Voltage applied usually controls the concentration of the redox species at the electrode surface and also the rate of the reaction. Nernst and Butler-Volmer equations paint a clear picture of these relationships. When diffusion controls the amount of current drawn, Fick's Law comes into play. The faradaic current generated in this case is related to the flux of the material at the electrode-analyte junction. Equation 22 is the Nernst equation, adapted from reference 46 showing the relationship between the applied potential and the concentration of the redox species [46].

$$E = E^{O} - \frac{RT}{nF} \ln \frac{C_R^O}{C_O^O} \tag{22}$$

- **R**- molar gas constant 8.314Jmol$^{-1}$K$^{-1}$
- **T**-absolute temperature K
- **n**- number of electron equivalent per mole of redox agent.
- $\mathbf{E^0}$- standard redox potential for the redox couple.
- **F**- Faraday's constant 96485 (C/equiv)
- $\mathbf{C_R^o}$- Concentration of the reduced form of the redox species at the electrode surface.

- $\mathbf{C_O^o}$- Concentration of the oxidized form of the redox species at the electrode surface.

Both peak potentials and peak currents can be determined and if the reaction is reversible then the peak separation is given by equation 23 [46].

$$\Delta E_p = E_{pa} - E_{pc} = 2.303\, {}^{RT}/_{nF} \tag{23}$$

The formal potential and the peak current are given by equations 24 and 25 respectively

$$E^o = \frac{E_{pc} + E_{pa}}{2} \tag{24}$$

$$i_p = 2.686 \times 10^5\ n^{3/2} A c^o\, D^{1/2} v^{1/2} \tag{25}$$

Where:

*A- Area of the WE*

*$v$- the scan rate*

*D- diffusion coefficient of the electroactive species*

Equation 26 is the Butler-Volmer equation, also taken from reference 46, and it gives the relationship between concentration, current and potential of an electrochemical system under study.

$$\frac{i}{nFA} = k^o\{C_O^o exp[-\propto \theta] - C_R^o exp[(1-\alpha)\theta] \tag{26}$$

Where: α- transfer coefficient, A is the electrode area, $k^0$ is the heterogeneous rate constant and $\theta = nF(E-E^0)/RT$.

Current flowing usually depends directly on the flux of material to the electrode surface. Creation of new redox species forces diffusion to occur either to or from the bulk of the solution.

This scenario is described by Fick's law, which states that the flux is directly proportion to the concentration; equation 27 is a summary of Fick's law.

$$\emptyset = -AD_o(\partial_{co}/\partial x) \quad (27)$$

Where: $D_o$ is the diffusion coefficient, x is the distance from the electrode surface and $\emptyset$ is the flux

**Potentiostat experiments**

Our research objective is to electrochemically synthesize lithium borohydride, a hydrogen storage material. This is an inexpensive route compared to the current one. Electrochemical transfer of $H^-$ to $B(OCH_3)_3$ to finally make $BH_4^-$ will serve as a breakthrough in finding an energetically cheaper source of $H^-$.

The major equipment used throughout this research was a PAR 273A model potentiostat that was connected to a specially constructed electroanalytical cell that contained: a Teflon cell body, a thin palladium foil as the working electrode (WE), a platinum coil as the counter electrode (CE), a silver wire as a pseudo- reference electrode (RE) and the plumbing attachments. Figure 20 represents a clear picture of the assembled cell.

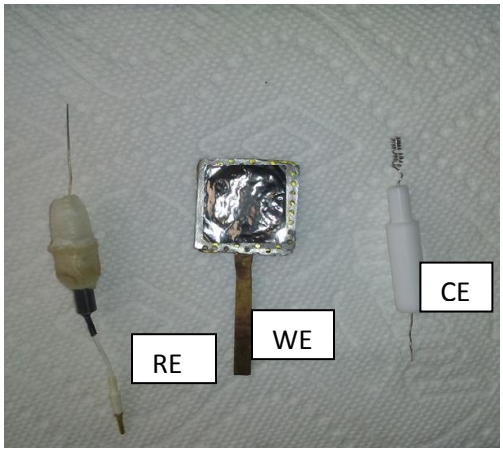


a) Electrodes

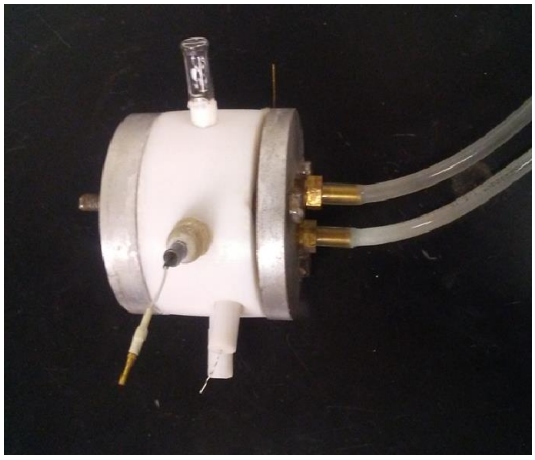

b) Cell body

**Figure 20:** Electrochemical cell components

The three electrodes were carefully connected to the potentiostat using alligator clips. The cyclic voltammetry experiments were done using a freshly prepared electrolyte that contained lithium perchlorate as the supporting electrolyte, acetonitrile as the solvent and trimethyl borate (TMB). All the reagents used in this research were purchased from Alfa Aesar, Acro Organics or Aldrich Chemicals. A 1 M $H_2SO_4$ solution was also prepared in the initial stages of the research and used as an electrolyte to electrochemically clean the Pd foil, since electrochemistry is a very sensitive technique whose results can be altered by the presence of even trace impurities. Electrochemical cleaning was done by sweeping the potential between -0.25 and +1.25 until a voltammogram suggesting clean Pd foil surface was obtained after which the foil was rinsed thoroughly with dry acetonitrile.

The intended product, lithium borohydride, is a moisture sensitive compound; because of that, the experiment was carried out in an inert atmosphere created first by obtaining dry acetonitrile from the solvent dispenser, and before the actual experiment, the electrolyte was purged with an inert gas (dry argon) using improvised apparatus.

Two different sets of solutions were prepared. First a blank electrolyte of 100 ml 0.1 M $LiClO_4$ in $CH_3CN$ was prepared by weighing carefully 1.0639 g of anhydrous $LiClO_4$ and dissolving it in 100 ml $CH_3CN$ in a volumetric flask. The final electrolyte was prepared by mixing 25 ml of pure TMB with 25 ml of the blank electrolyte resulting in an electrolyte containing 4.44 M $B(OCH_3)_3$ and 0.05 M $LiClO_4$ in acetonitrile.

In establishing the reference electrode potential of the silver wire, a CV experiment using a 5 mM solution of ferrocene in the conducting medium and silver wire as the working electrode was done. The range between the reduction potential and the oxidation potential of the electrolyte solvent was established by running a CV experiment on the blank electrolyte over a range of different potentials. The blank electrolyte contained only 0.1 M $LiClO_4$ in $CH_3CN$. This helped to establish the electrochemical window of the solvent.

To determine the effect of TMB on the electrochemical behavior of the blank electrolyte, TMB + $LiClO_4$ + $CH_3CN$ was now used instead of the blank electrolyte and a CV experiment run within the established potential window. In an attempt to establish whether $B(OCH_3)_3$ can accept a hydride ion transferred to it electrochemically, a CV experiment was performed, but this time hydrogen gas was supplied to the back side of the Pd foil from a hydrogen tank at a precisely determined pressure simultaneously.

Figure 21 shows the experimental set-up.

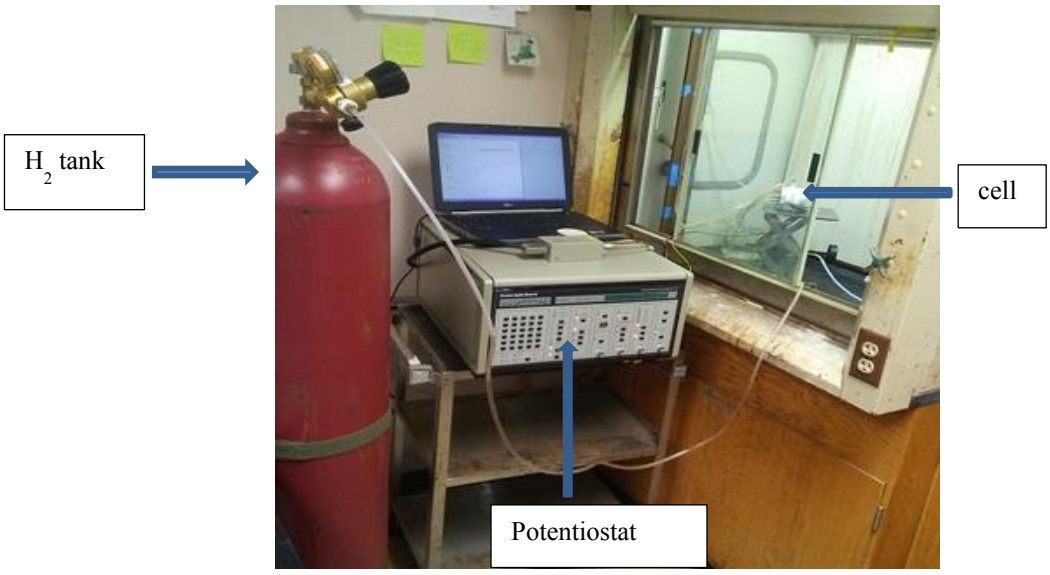


**Figure 21**: Experimental set-up for cyclic voltammetry

To make detectable amount of the borohydride, bulk electrolysis was done through a potentiostatic experiment for 2 hours where the working electrode potential was -2.75 V.

**The two-compartment cell**

A two-compartment electrochemical cell with Nafion (N115) that was obtained from the fuel cell store was used as a separator of catholyte and the anolyte reagents, so as to allow selective movement of $Li^+$ to the working electrode, was designed as shown in Figure 22 below.

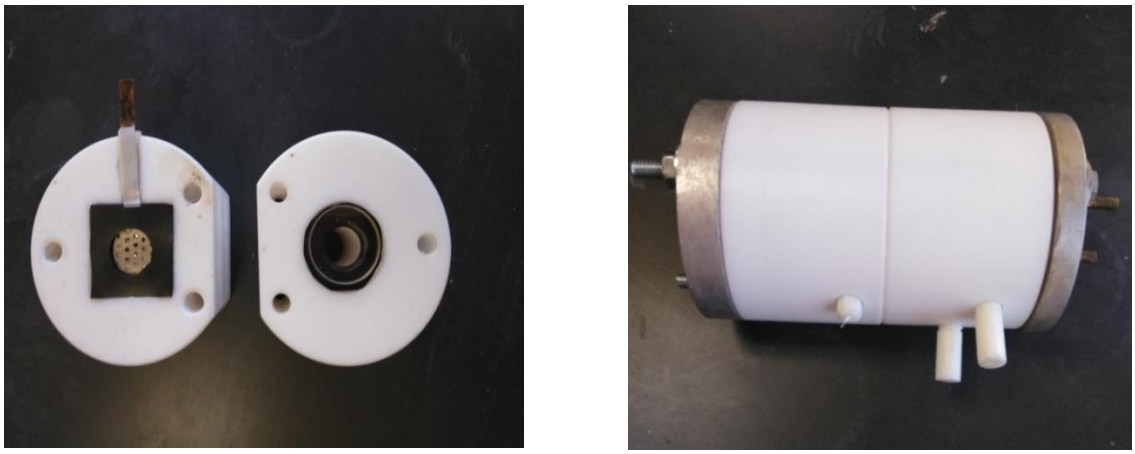

**Figure 22:** Two compartment cell assembly

**The Nafion membrane**

Figure 23 taken from reference 47 shows the repeating structural units comprising the Nafion polymeric membrane.

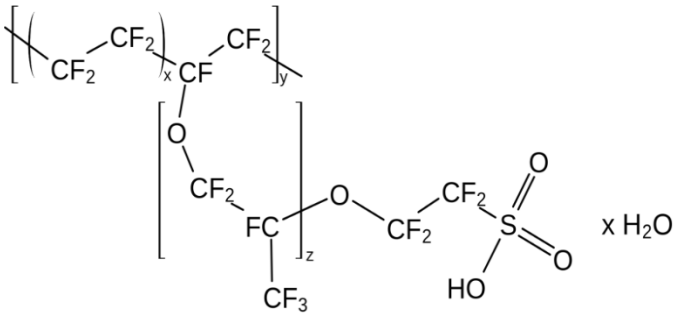


**Figure 23**: Nafion membrane

It is a sulfonated tetrafluoroethylene co-polymer with the following properties:

- Conductive to cations
- Resistant to chemical attack
- Able to withstand high temperatures

A 4 cm by 4 cm piece of the membrane was carefully cut and soaked in a 2 M $LiClO_4$ solution in water and at the same time the pH of the solution monitored using the pH meter. It was observed that the pH of the solution dropped drastically from 9.61 to 1.70, an indication of ion exchange between the protons in the membrane and the lithium ions in the solution. The procedure was repeated until no more change in pH was observed. The membrane was then transferred into a watch glass and heated in an oven at 119$^{o}$C with changes in mass closely monitored at intervals of 30 min each until a constant mass was attained. The mass was found to have decreased by 13.6% after heating. Finally, the membrane was boiled in acetonitrile for 1 hour prompting its mass to increase again by 8.8% and was ready for mounting. The main reason for using the membrane was to act as a barrier between the electrode reagents and also products formed at the respective electrodes in this way the concentration of the intended product could be increased.

The cathode compartment was filled with 8 ml of 0.05 M $LiClO_4/CH_3CN$ and 4.4 M TMB while the anode compartment was filled with 5 mM of ferrocene in 0.1 M $LiClO_4/CH_3CN$ as shown in Figure 24.

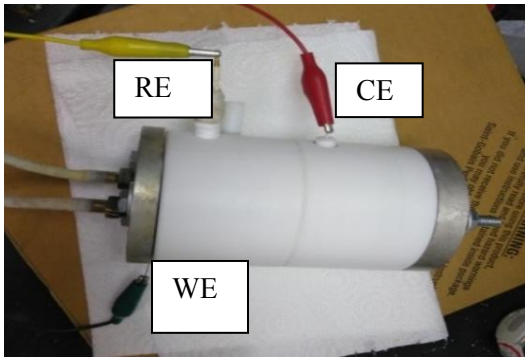


**Figure 24:** CV experimental set-up for ferrocene, 0.001 to -2.75 V, 3 scans and 50mV/s**.**

## 2.2 Infrared spectroscopy

Spectroscopy is the study of matter and its interaction with electromagnetic radiation. IR spectroscopy is largely confined to molecular vibrations. For a molecule to absorb IR radiation, it must undergo a net change in dipole moment. The intensity of an absorption band depends on the change in the dipole moment of the bond and the number of the specific bonds present. Dipole moment is due to bond length and the charge difference between the two atoms. The charge difference is derived from the electronegativity values of the atoms involved. Molecules such as $O_2$ and $N_2$ do not absorb IR radiation because they don't have an electronegativity difference. Theoretically, an oscillating or vibrating covalent bond of a molecule due to change in dipole moment creates a varying electromagnetic field. When infrared radiation encounters this oscillating dipole of the EM field, generated by the oscillating dipole of the same frequency, the two waves couple and the radiation is thus absorbed, increasing the amplitude. Determining the frequencies of the coupled wave allows one to determine the bonds present in a molecule. IR spectroscopy is used to give an intelligent guess of the chemical structure of a compound, because the various absorption peaks having specific wave numbers are characteristic of various functional groups. The infrared portion of the electromagnetic spectrum includes three regions; the near-, mid and far- infrared, named for their relation to the visible spectrum. The far-infrared, approximately 400-10 $cm^{-1}$, lying adjacent to the microwave region, has low energy and may be used for rotational spectroscopy. The mid-infrared, approximately 4000-400 $cm^{-1}$, may be used to studying the fundamental vibrations and associated rotational-vibrational structure. The higher energy near-IR, approximately 14000-4000 $cm^{-1}$ can excite overtone or harmonic vibrations. The bonds

can vibrate with stretch motions or bending motions. The stretching motions can either be asymmetric or symmetric. Radiation wavelengths in the infrared region are represented in terms of wavenumbers, which is the number of waves per centimeter. The wavenumbers are directly proportional to the energy of the IR radiation meaning that the higher the wavenumber the higher the energy of the radiation [48]. The spectrum is split into two regions: the functional group region and the fingerprint region. Two different functional groups may have similar absorption in the functional group regions but different fingerprint regions. Bending vibrations are usually found in the finger print region. Figure 25 shows the two regions, along with functional group information.

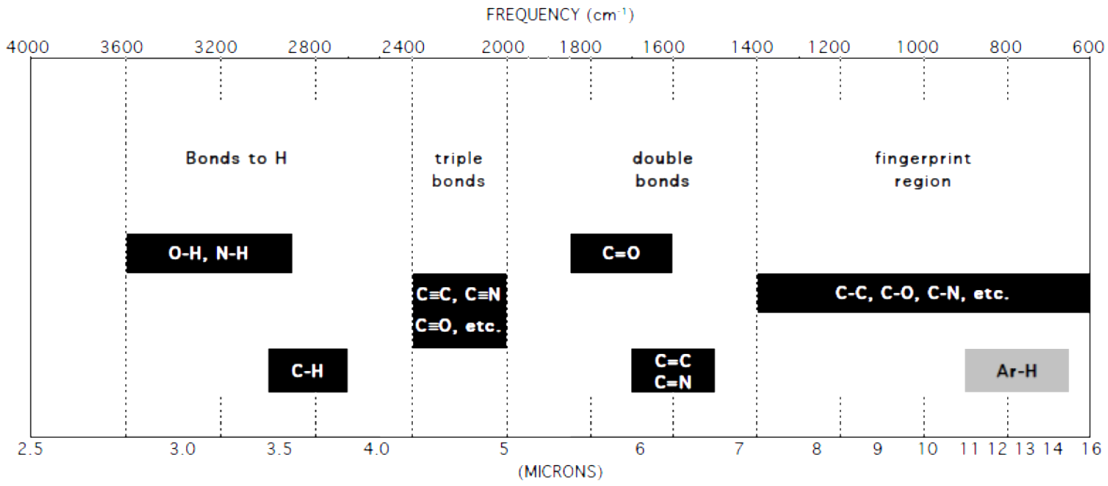


**Figure 25:** IR absorption bands [48].

Bond vibrational energies vary as one moves horizontally across the graph. Bond strength and atom masses of the bonded atoms determine the bonding energy [48].

Figure 26 shows a schematic diagram of an FT-IR spectrophotometer

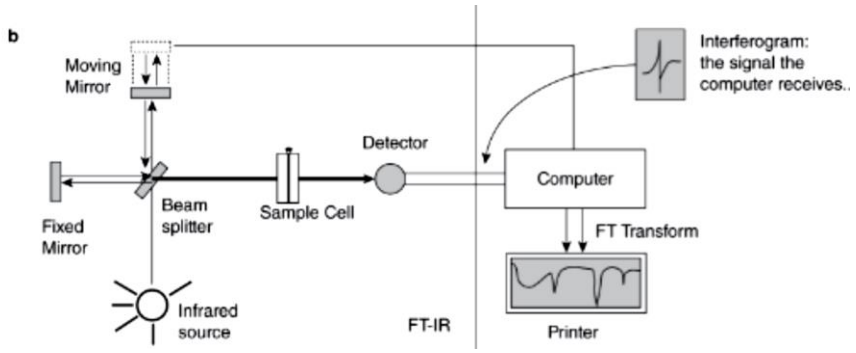


**Figure 26:** FT-IR spectrophotometer [48].

In this work, IR spectroscopy was used as an analytical tool to qualitatively determine the presence or rather the formation of B-H bonds in the product. Biljana et al. report that B-H vibrations occur at 2225, 2293, and 2640 $cm^{-1}$. Figure 27 below is an IR spectrum of experimental product sodium borohydride and pure sodium borohydride, prepared as a KBr pellet, taken from reference 49.

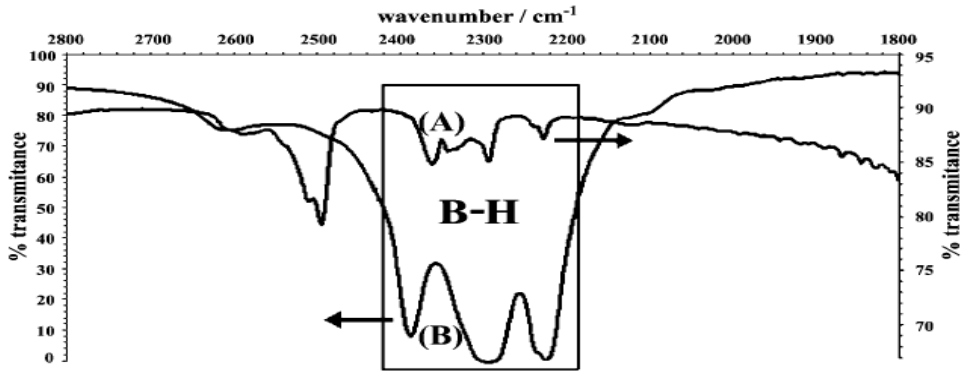


**Figure 27:** IR spectra of reaction product sodium borohydride (A) and that of pure sodium borohydride (B) [49].

IR 200 spectrometer was used to analyze the electrolysis product to see if any B-H compound was indeed formed. Three different sets of spectroscopic analysis were done. First the IR spectra of commercial lithium borohydride dissolved in THF was taken so that it could be used as the control experiment, then the spectra for the electrolyte containing TMB + $LiClO_4$ + $CH_3CN$ was taken before and after 2 hours electrolysis. The two compartment cell experimental products were also analyzed using this technique.

**2.3 Proton NMR**

Nuclear Magnetic Resonance, NMR, is used to study different properties of atomic nuclei and more specifically molecular structure of organic compounds. A nucleus with spin and charge when placed in an external magnetic field behaves as a magnet. Only those nuclei with net spin can be studied by NMR. In this analytical technique, a magnetic field is applied to a nuclei and the amount of energy required to flip the nuclear spin into an excited state is measured. This leads to an NMR spectrum that provides signals or peaks representing these energies. In this work, the proton NMR of B-H bonds that were suspected to be formed was used as a confirmatory test whether indeed a hydride ion was transferred to the boron atom. First, the proton NMR spectrum of commercial lithium borohydride was taken, followed by the NMR spectrum of the electrolyte before and after electrolysis.

## Chapter 3: Results and discussion

### Results and discussion

First, a potentiostat was used to determine the performance of the palladium foil electrode in 1 M $H_2SO_4$ wih $H_2$ application and the resultant voltammogram obtained as shown in Figure 28 below.

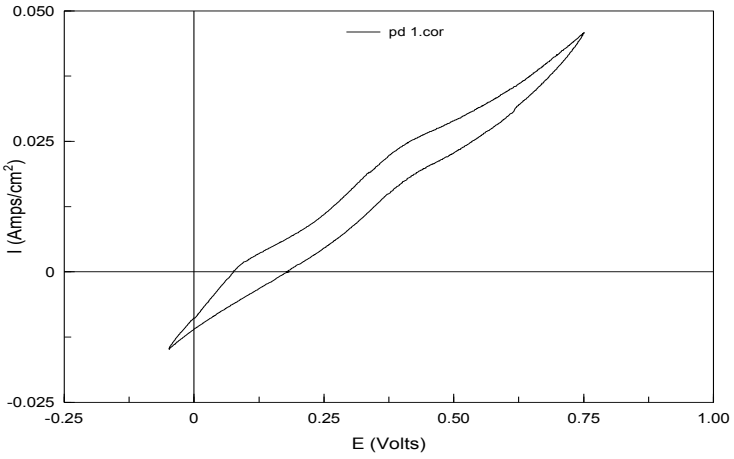


**Figure 28:** Cyclic voltammogram for 1 M $H_2SO_4$ using palladium foil as the working electrode.

The same potentiostat was used to determine the potential window of acetonitrile as the solvent. This was necessary to show how far one can sweep negative because the objective of this work was to hydrogenate TMB to form borohydride. Hydriding usually occurs at the negative potentials. A clean cyclic voltammogram indicated no electrochemical activity for acetonitrile within the chosen window of 0.001 to -2.75 V.

After several attempts, the following voltammogram in Figure 29 was obtained.

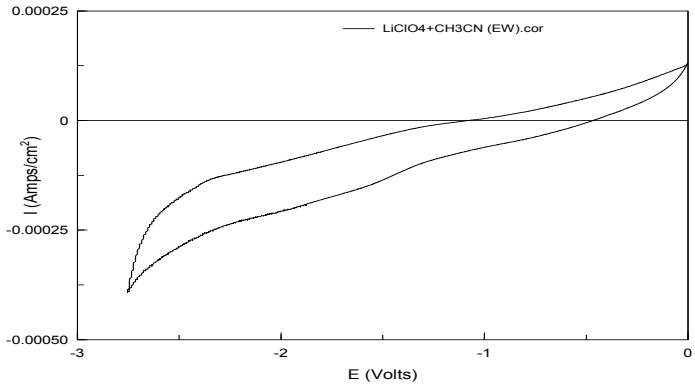


**Figure 29:** Cyclic voltammogram for 0.1 M $LiClO_4$ + $CH_3CN$. Sweep rate 50 mV/s and 3rd cycle, Pd foil as WE, Pt coil as CE and Ag wire as the RE under argon purge

It is clear that between 0.001 and -2.75 V, there was little or no faradaic activity and even the small current observed can be attributed to capacitative effects. The range 0.001 to -2.75 V was established as the workable range for our purposes. This was good and in agreement with the intended objective of this research. The voltammogram of 5 mM ferrocene in the conducting electrolyte media using Ag wire as a working electrode showed a reasonably reversible redox reaction for ferrocene and thus a reference electrode potential for $Ag/AgClO_4$ was established at 0.3 V vs NHE as shown in Figure 30.

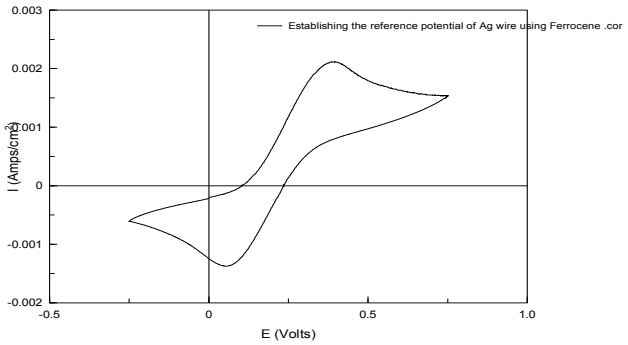


**Figure 30**: Reference electrode potential of ferrocene/silver wire

The electrochemical effects of trimethyl borate on the blank electrolyte were investigated. A cyclic voltammogram of 0.05 M $LiClO_4$ + $CH_3CN$ + TMB was done to serve as the control experiment for the hydriding process. The voltammogram in Figure 31 didn't show much difference from that of the blank electrolyte as far as current drawn was concerned. However, some electrochemical activity was observed around 1.2 V indicating the presence of an impurity, methanol being one of the major impurities in TMB or possibly molecular oxygen from background air.

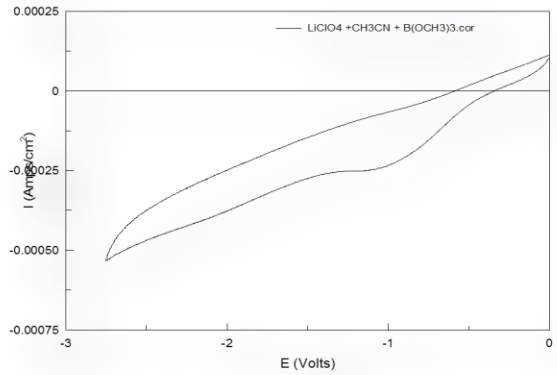


**Figure 31:** Cyclic voltammogram for 0.05 M $LiClO_4$ + $CH_3CN$ + 4.4 M TMB. Sweep rate 50 mV/s and 3 scans, Pd foil as WE, Pt coil as CE and Ag wire as the RE under argon purge

The application of hydrogen gas at a pressure of 1.02 atmospheres from the back side of the cell was now investigated and its effects on the amount of current drawn noted. A cyclic voltammogram of 0.05 M $LiClO_4$ + $CH_3CN$ + 4.4 M TMB + $H_2$ at a pressure of 1.02 atmospheres supplied from the backside of the cell was taken at a scan rate of 50 mV/s, 3 scans between potential sweeps of 0.001 to -2.75 V. The voltammogram in Figure 32 showed a remarkable increase in current, suggesting that the application of hydrogen gas had an effect; possibly hydriding of the TMB.

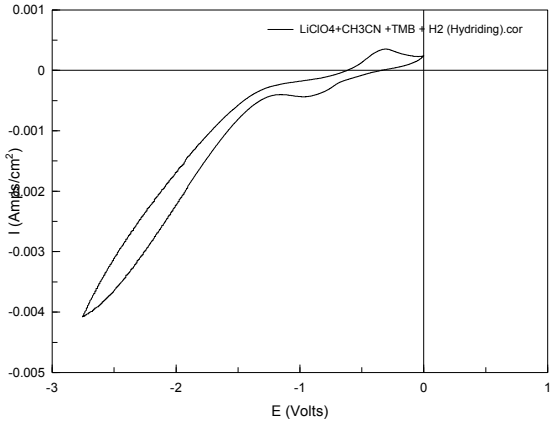


**Figure 32:** Cyclic voltammogram for 0.05 M $LiClO_4$ + $CH_3CN$ + 4.4 M TMB + $H_2$ (1.02 atm) Sweep rate 50 mV/s and 3 scans, Pd foil as WE, Pt coil as CE and Ag wire as the RE under argon purge.

Between 0.0 and -1.0 V, a reversible process is observed and is attributed to the electrochemical activity of oxygen gas. An overlay of the three previous voltammograms is shown in Figure 33.

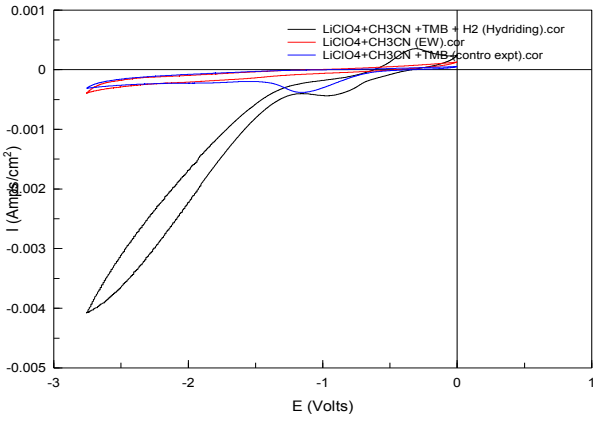


**Figure 33:** An overlay of voltammograms showing the effect of $H_2$ and TMB

Due to the continued reproducibility of these results more than 10 times, the question of whether $H^-$ was attaching itself to the TMB to make any B-H bonds needed an answer. It was decided to perform a bulk electrolysis to synthesize lithium borohydride and further analyse it using IR and NMR. A potentiostatic experiment for 2 hours was performed while holding the WE potential at -2.75 V and using the same electrolyte and cell as described earlier in this work. Figure 34 is the current versus time graph obtained over the 2-hour electrolysis

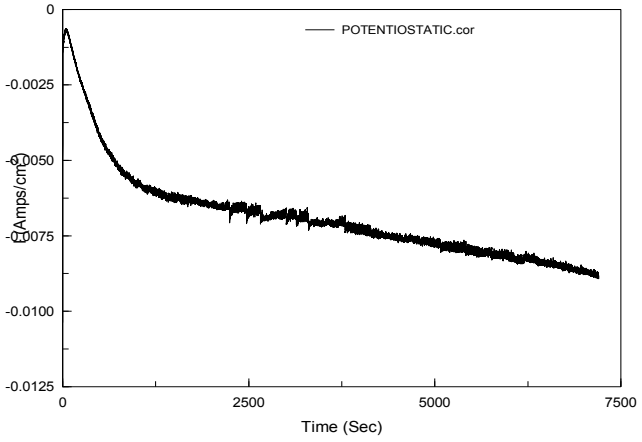


**Figure 34:** Potentiostatic experiment, WE electrode held at -2.75 V, $H_2$ at a pressure of (1.02 atm) for 2 hours.

After the time had passed, the electrolyte was sampled and analyzed. Infrared spectroscopy was used. First, IR spectra of commercial lithium borohydride and sodium trimethoxy borohydride were taken in order to provide a reference spectrum for the formation of B-H bonds. All the solids were dissolved in ammonium hydroxide. Borohydride species are known to be stable in strong alkali, where the proton concentration is very low and cannot initiate hydrolysis of the B-H bonds.

Figure 35 is an IR spectrum of the solvent used (concentrated aqueous ammonia) and Figures 36 and 37 are the IR spectra of lithium borohydride and sodium trimethoxy borohydride, respectively.

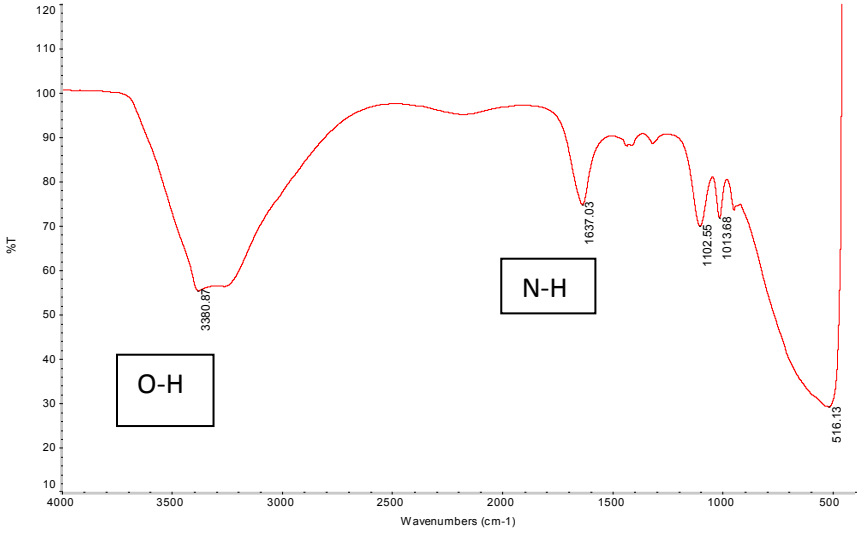


**Figure 35:** IR spectra of ammonium hydroxide solution.

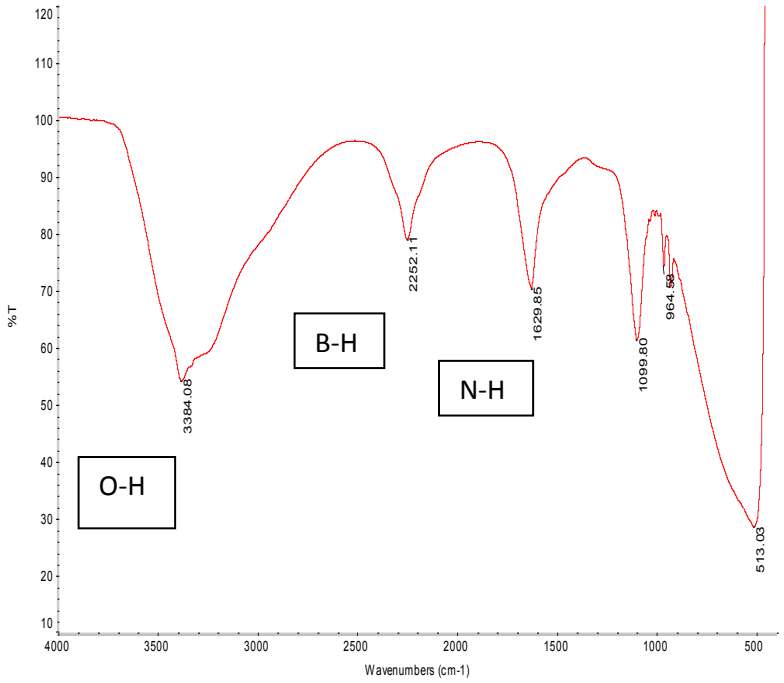


**Figure 36:** IR spectra of 0.5 M lithium borohydride in ammonium hydroxide.

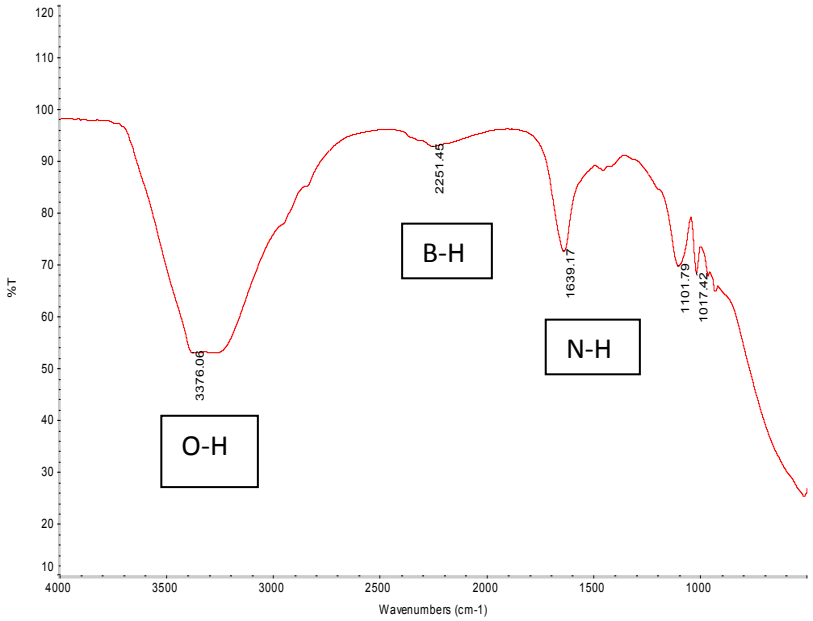


**Figure 37:** IR spectra of 0.5 M sodium trimethoxy borohydride in ammonium hydroxide.

The B-H stretch is more pronounced in lithium borohydride than in sodium trimethoxy borohydride because of the difference in the number of B-H bonds on the respective molecular species. With these spectra in-hand, the IR spectra of the electrolyte before and after electrolysis were taken. Figure 38 is an IR spectrum of the electrolyte (0.05 M $LiClO_4$ + $CH_3CN$ + 4.4 M TMB) before electrolysis, which was used for comparison purposes, while Figure 40 is the spectrum of the electrolysis product.

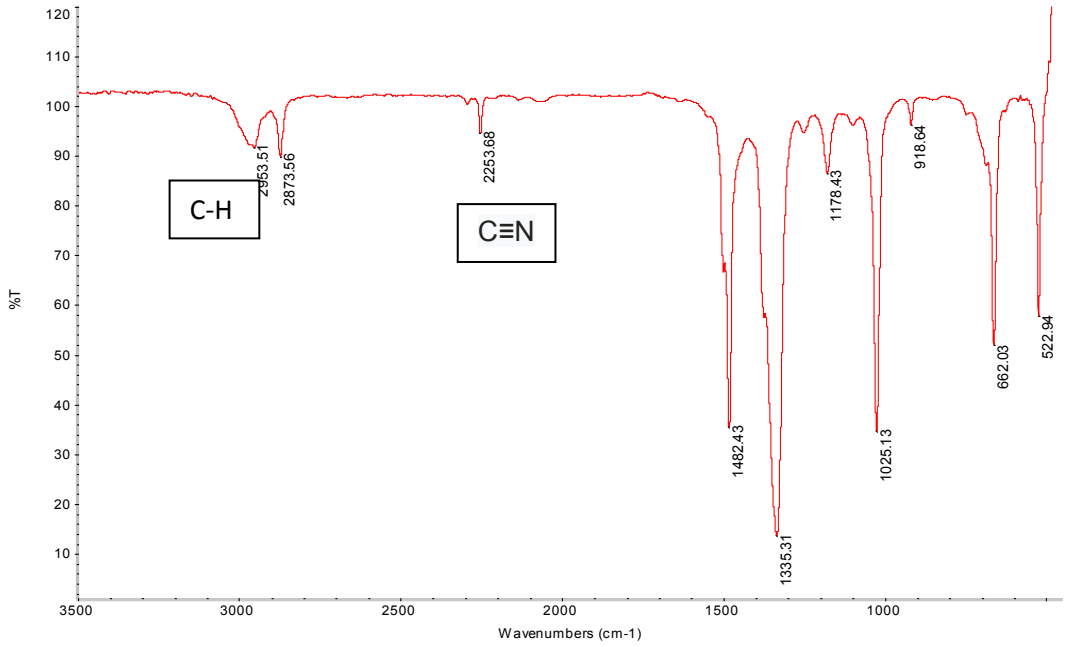


**Figure 38:** IR spectrum of the electrolyte (0.05 M $LiClO_4$ + $CH_3CN$ + 4.4 M TMB) before electrolysis

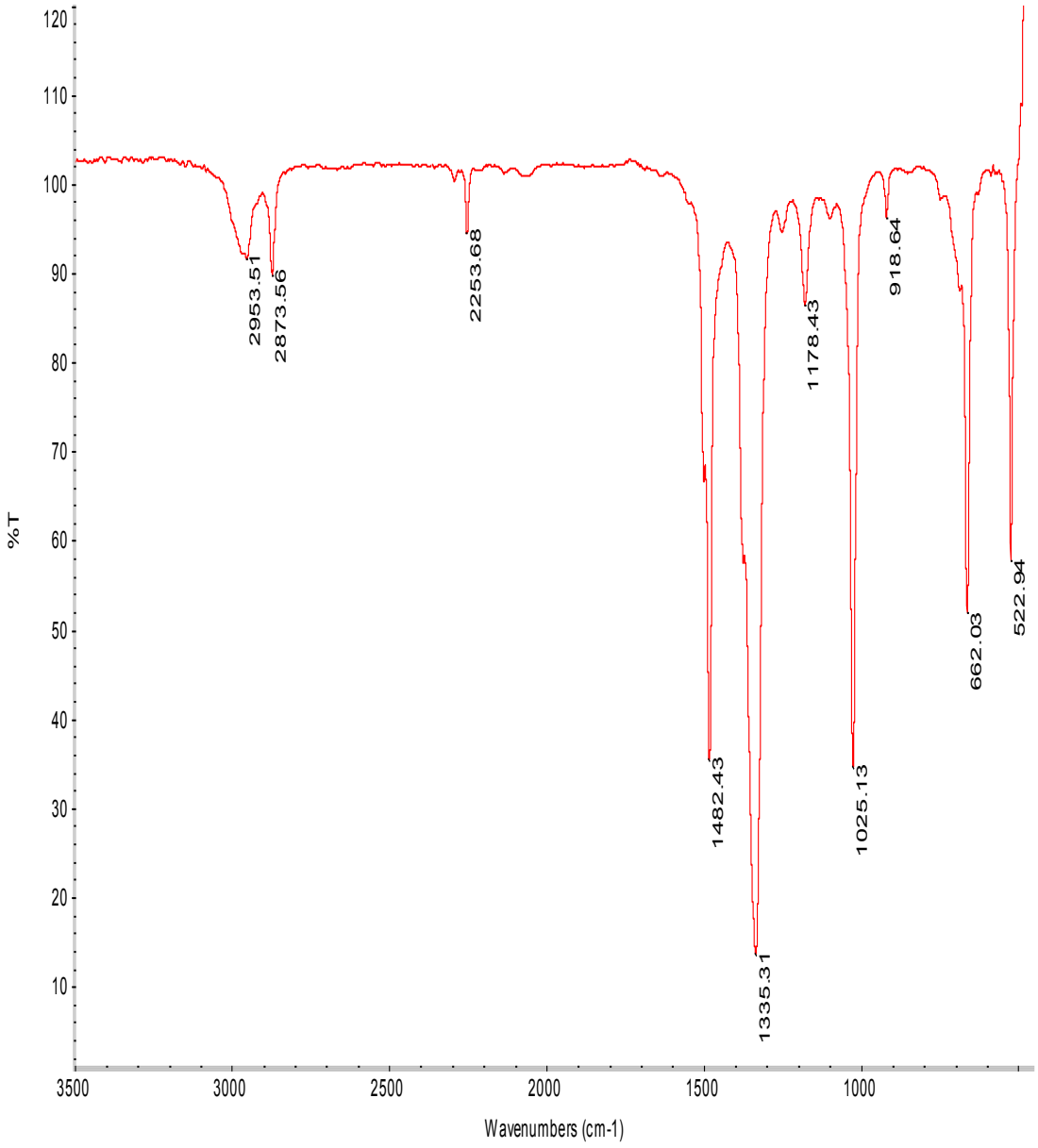


**Figure 39**: Expanded IR spectrum of the electrolyte (0.05 M $LiClO_4$ + $CH_3CN$ + 4.4 M TMB) before electrolysis

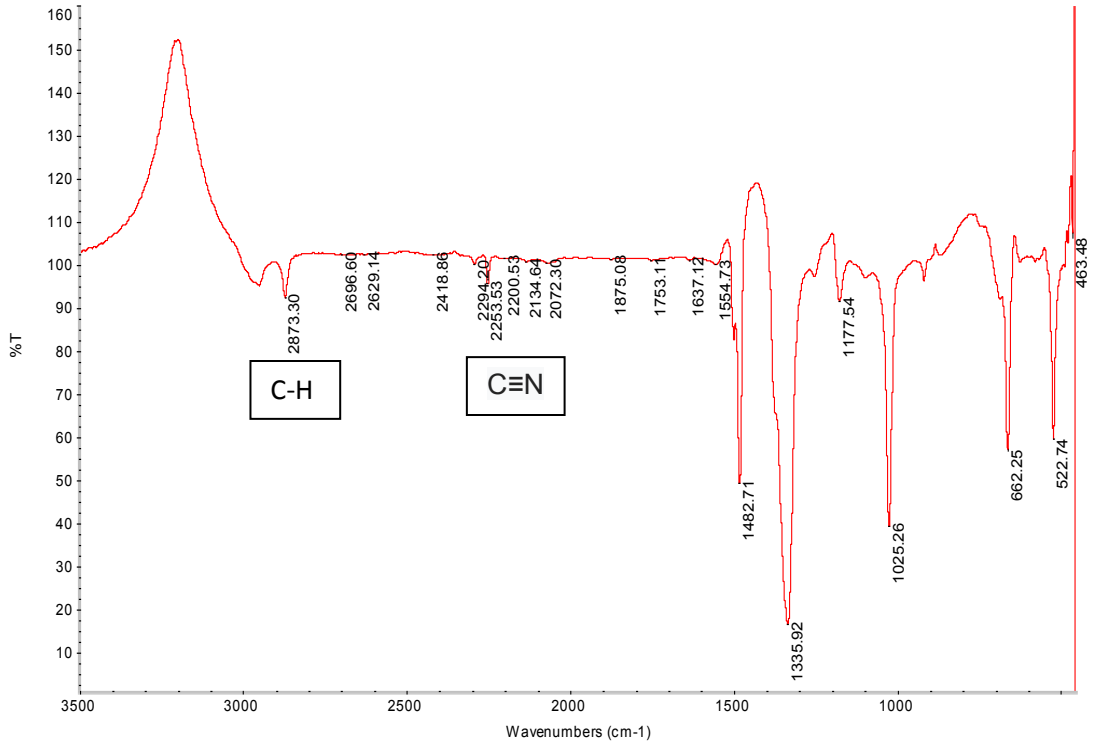


**Figure 40:** IR spectrum of 0.05 M $LiClO_4$, 4.4 M TMB in $CH_3CN$ after 2- hour electrolysis at -2.75 V vs $Ag/AgClO_4$ under $H_2$ pressure.

The spectrum in Figure 40 was expanded out to between 2300-2500 wavenumbers, where some traces of weak B-H stretches were found. On matching the spectra of the product with the reference sample, a similar vibration band was observed at 2250 $cm^{-1}$. Further probing was done to ascertain whether the stretch was due to the nitrile group of $CH_3CN$ or B-H stretch. A proton NMR was done to see if there were H-B chemical shifts.

First the proton nmr spectrum of the electrolyte before electrolysis was taken to act as a reference sample. Figure 41 is the proton nmr of 0.05 M $LiClO_4$ + $CH_3CN$ + 4.4M TMB. The peak at 2.0 ppm is due to acetonitrile and the peak at 3.6 ppm is due to TMB.

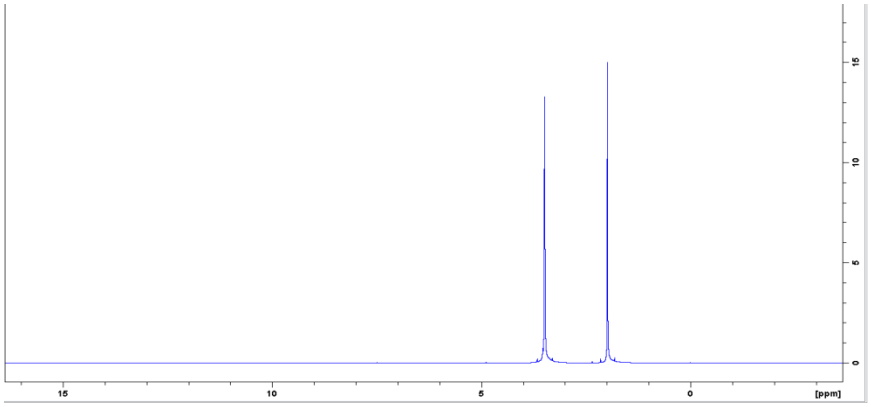


**Figure 41:** Proton nmr of 0.05 M $LiClO_4$ + $CH_3CN$ + 4.4 M TMB in $CDCl_3$

Figure 42 is the proton nmr of the 2-hour electrolysis product.

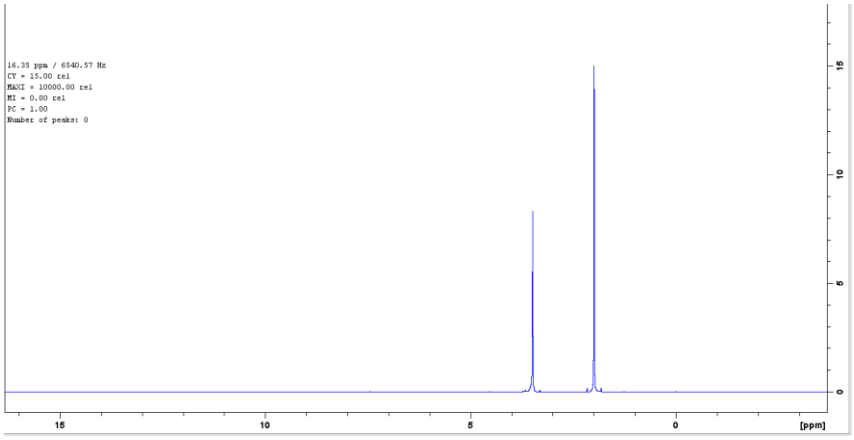


**Figure 42:** Proton nmr spectrum of the 2 h. electrolysis product, including $H_2$, TMB, $LiClO_4$ and $CH_3CN$ in $CDCl_3$.

The downfield peak has lower intensity compared to the upfield one, suggesting a 50% consumption of TMB.

From the IR and NMR results, the cause of the observed electrochemical activity was not clear. According to the manufacturers, one of the major impurities of TMB is methyl alcohol and therefore it was necessary to carry out electrochemistry of methyl alcohol under the same conditions in order to ascertain its possible contribution to the observed results. Cyclic voltammograms were obtained and compared to the voltammogram in Figure 31. The results were similar as far as current drawn was concerned. Figure 43 represents the overlaid cyclic voltammograms obtained from the analysis of 40 mM of methanol with and without application of hydrogen gas under pressure in $LiClO_4$/ $CH_3CN$.

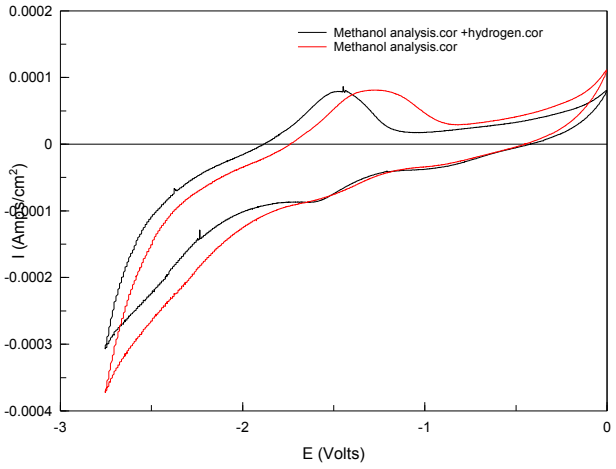


**Figure 43:** Cyclic voltammogram for 40 mM methanol on Pd foil in $LiClO_4/CH_3CN$.

Application of hydrogen gas from the back side of the electroanalytical cell did not show much difference. The minimal current when hydrogen gas was applied confirmed that the methanol impurity in TMB would have no role in the electrochemical activity observed when TMB is added.

It is speculated that some hydriding process is taking place and some hydrogen boron bonds are forming but in very low concentrations that cannot be sensed by IR.

Coulometric calculation below is a confirmation of the negligible amount of the B-H compound that might have formed for the 2 hours.

$$\frac{i \cdot t}{nF \cdot V_{cell}} = Molarity\ of\ the\ product\ formed.$$

Where *i- current in amperes*

*t - time in seconds*

*F- Faraday's constant*

*V- cell volume in liters.*

Over two hours, the following concentration would be formed at 100% coulombic efficiency.

$$\frac{0.01 \times 2 \times 60 \times 60}{1 \times 96485 \times 7 \times 10^{-3}} = 0.1\ \text{M}$$

The IR spectrometer didn't sense the B-H bonds, as this was attributed to the low concentration of the product formed. Analysis of 0.1 M and 0.5 M of commercial sodium trimethoxy borohydride ($NaBH(OCH_3)_3$) resulted in the IR spectra shown in Figures 44 and 45 respectively.

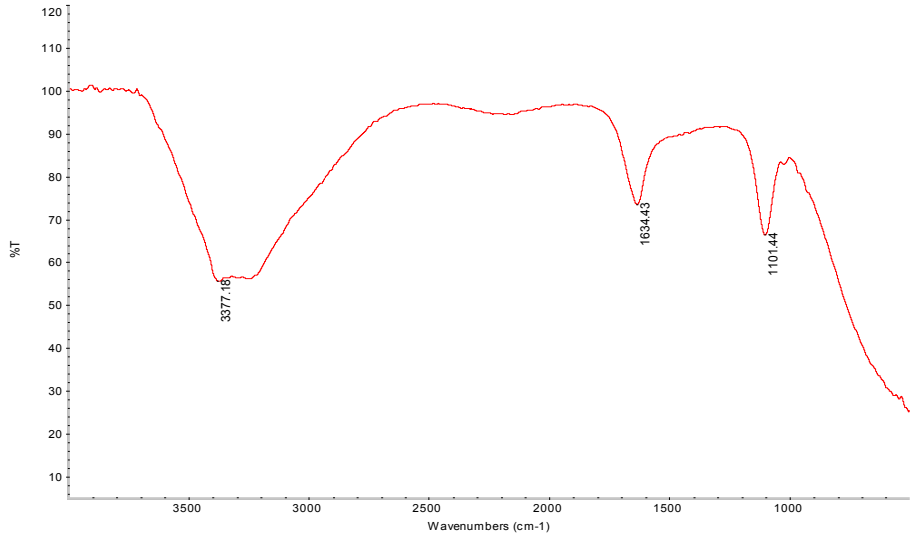


**Figure 44:** IR spectrum of 0.1M NaBH $(OCH_3)_3$ in ammonium hydroxide.

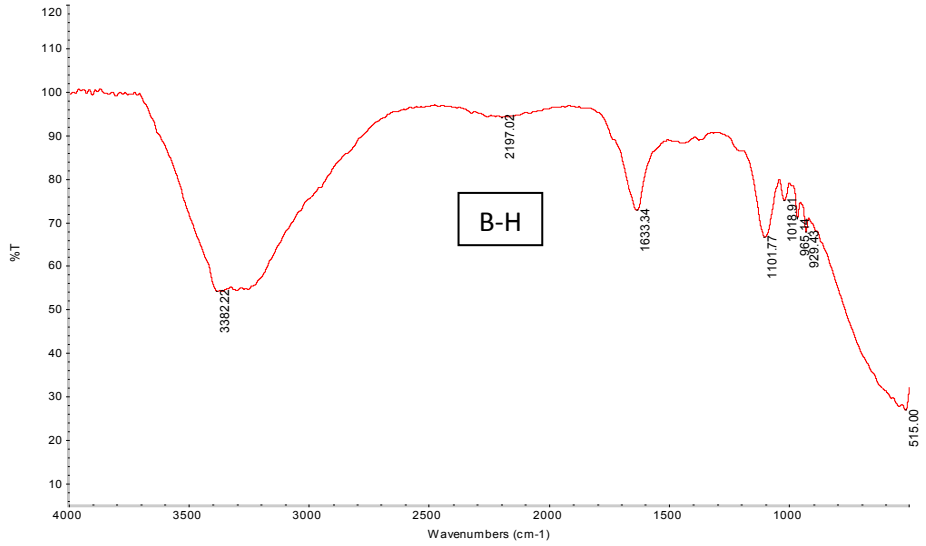


**Figure 45:** IR spectrum of 0.5 M NaBH$(OCH_3)_3$ in ammonium hydroxide.

The calculations clearly indicate that if one wants more of the product, then the experimental time must be increased. To investigate this, the experiment was repeated, but this time for 9.5 hours so that slightly more than 0.5 M of the borohydride can form.

The solubility of lithium borohydride in acetonitrile is very low compared to THF. Possibly the amount of the borohydride formed does not dissolve enough in the acetonitrile to achieve detection levels; it is also possible that it reacted with background moisture, as it is very sensitive compound to neutral water.

This prompted the use of THF as a solvent for the electrosynthesis of lithium borohydride. A solution of 0.1 M $LiClO_4$ + THF was prepared and cyclic voltammetry experiments done as described earlier with acetonitrile. The following cyclic voltammograms summarizes the findings.

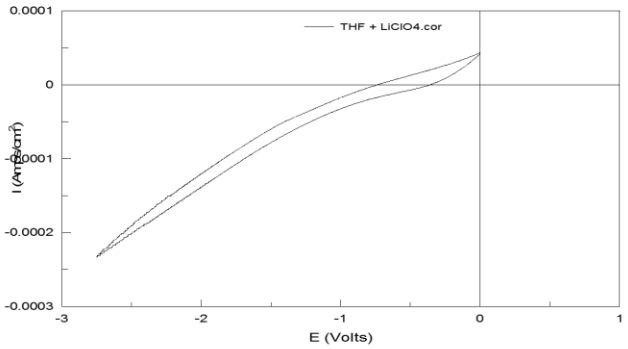


**Figure 46:** Cyclic voltammogram for 0.1 M $LiClO_4$ in THF.

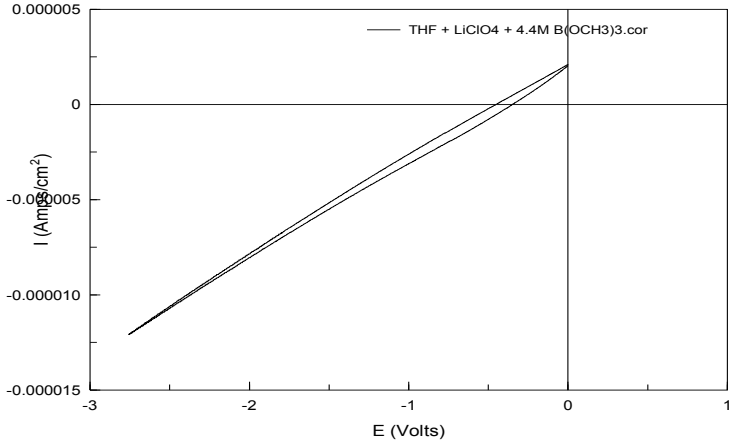


**Figure 47:** Cyclic voltammogram for 0.05 M $LiClO_4$ + THF + 4.4 M B $(OCH_3)_3$

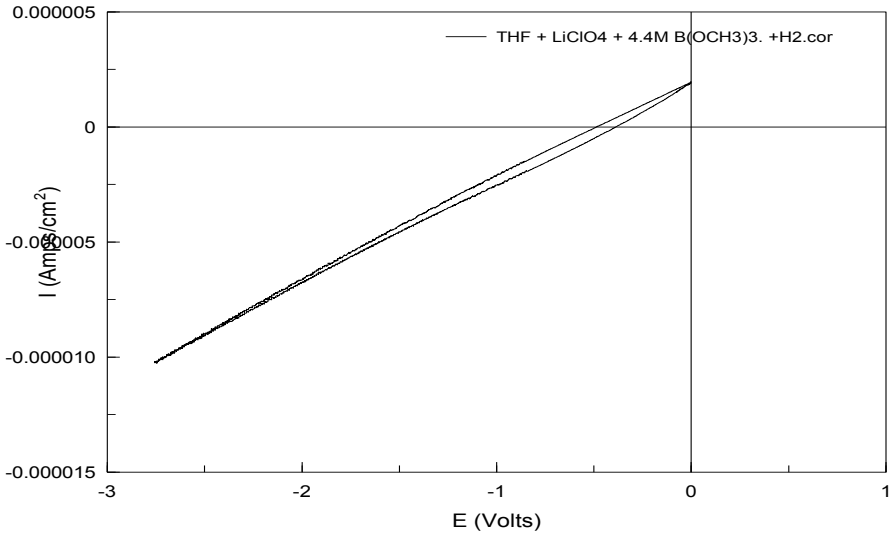


**Figure 48:** Cyclic voltammogram for 0.05 M $LiClO_4$ + THF + 4.4 M $B(OCH_3)_3$ + $H_2$ at high pressure.

The results showed that very little electrochemistry was taking place in each case and therefore no product after extended electrolysis could be expected.

Figure 48 shows that the addition of TMB reduced the current even further because it adsorbed on the Pd electrode. To determine the electrochemical compatibility of THF and $LiClO_4$, a different supporting electrolyte was used. A solution of 0.1 M tetrabutylammonium perchlorate (TBAP) in THF was prepared and and its cyclic voltammogram obtained.

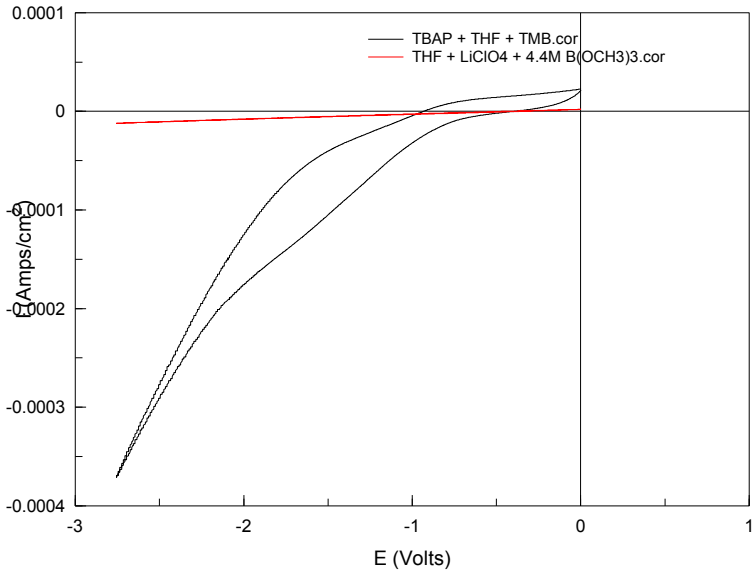


**Figure 49:** Cyclic voltammograms of THF in 4.4 M TMB with 0.05 M of different supporting electrolytes, TBAP and $LiClO_4$.

The voltammogram in Figure 49 clearly shows that there were conductivity issues when THF and $LiClO_4$ were used. This was enough to disqualify the use of THF in the electrosynthesis of lithium borohydride. The observed results can be attributed to either nondissociation of lithium perchlorate in the THF or there could be kinetic barriers.

The low boiling point of both acetonitrile and THF could not allow the experiment to be conducted at raised temperatures. For acetonitrile, a different concentration of TMB was used, but the difference was not significant.

Mixing of electrode reagents during electrolysis can either suppress the formed product or even lead to decomposition of it. A two compartment cell with Nafion as the separating membrane was suggested in order to improve the yield of the product and at the same time keep it in the cathode compartment. The cyclic voltammogram in Figure 50 below confirmed the conductivity of the membrane and opened the opportunity for bulk electrolysis under application of hydrogen from the backside of the cathode compartment.

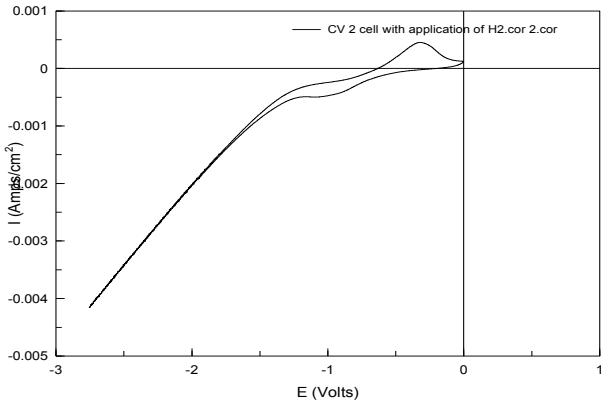


**Figure 50:** Cyclic voltammogram, 3rd scan, for the two cell compartment containing 5 mM ferrocene in the counter electrode compartment. Same $LiClO_4$ in $CH_3CN$ supporting electrolyte in both compartments. The cathode compartment was 4.4 M TMB.

The reversible redox behavior is due to the presence of oxygen, an indication that even after purging the solution with dry argon gas, not all oxygen gas was suppressed. After a 30 min cell trial, a potentiostatic experiment was immediately set at -2.75 V for 10 h. After 1.5 h the current drawn was seen to be decreasing with time as shown in Figure 51.

The experiment was stopped and the contents of the cathode compartment inspected and found that the membrane didn't act as the barrier as intended.

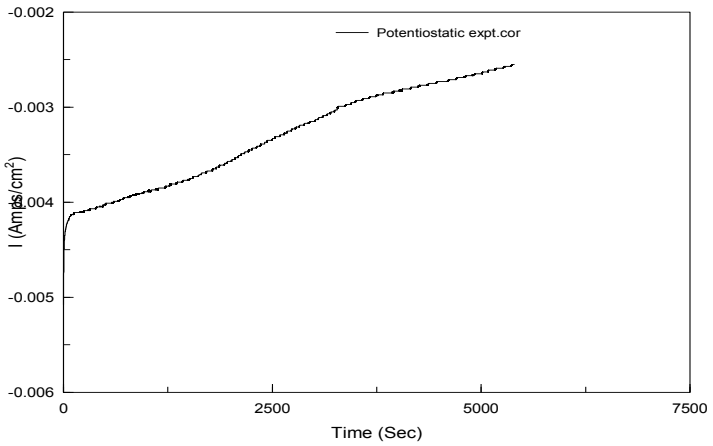


**Figure 51:** Potentiostatic experimental for dual compartment cell containing 4.4 M TMB in the WE compartment and 5 mM ferrocene in the CE compartment. $LiClO_4/CH_3CN$ supporting electrolyte in both compartments.

The contents of the cell on both sides of the membrane were found to be green in color, indicating the decomposition of ferrocene and the migration of the ferrous ions from the anode side to the cathode side. This was a signal that the membrane failed to perform its function of separating reagents between the anode and cathode side.

The use of ferrocene was abandoned and methanol was instead proposed to supply reducing equivalents to the anode side.

**The use of methanol on the anode side of the 2-compartment cell**

Instead of ferrocene, 0.5 M of methanol in 0.1 M $LiClO_4/CH_3CN$ was used in the anode compartment, while the cathode side was filled with 4.4 M TMB in 0.05 M $LiClO_4/CH_3CN$. A quick CV experiment without hydrogen application was done and the cell conductivity and stability confirmed through the voltammogram in Figure 52

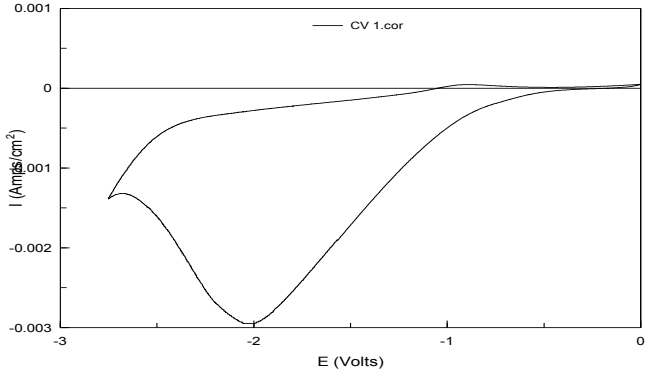


**Figure 52:** CV curve, 3rd scan, at 0.001 V to -2.75 V for the two compartment cell containing 0.5 M methanol in 0.1 M $LiClO_4/CH_3CN$ in the counter electrode compartment and 4.4 M TMB in 0.05 M $LiClO_4/CH_3CN$ in the WE compartment. Voltammetric activity observed at around -2 V is possibly due to methanol that has already permeated the Nafion membrane .

Another CV experiment was performed under application of hydrogen at a pressure of about 1 atm from the back side of the cathode compartment. The resulting voltammogram is shown in Figure 53.

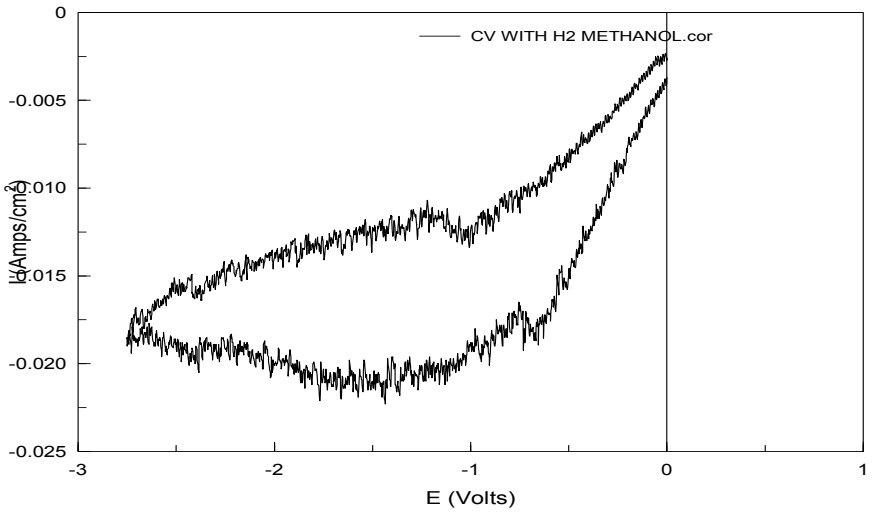


**Figure 53:** CV, 3rd cycle, at 0.001 V to -2.75 V, 50 mV/s, 1.02 atm $H_2$, for 0.5 M methanol in 0.1 M $LiClO_4/CH_3CN$ the counter electrode compartment.

A tremendous increase in current was noted, confirming earlier results obtained in the one compartment cell of increase in current whenever hydrogen is applied at a pressure. The voltammogram appears noisy due to the instability of the solution in the cell attributed to the hydrogen pressure that made the foil electrode to oscillate or possibly evolution of methane.

An overlay of CV curves shown in Figure 54 is a clear indication of the effect of applying hydrogen.

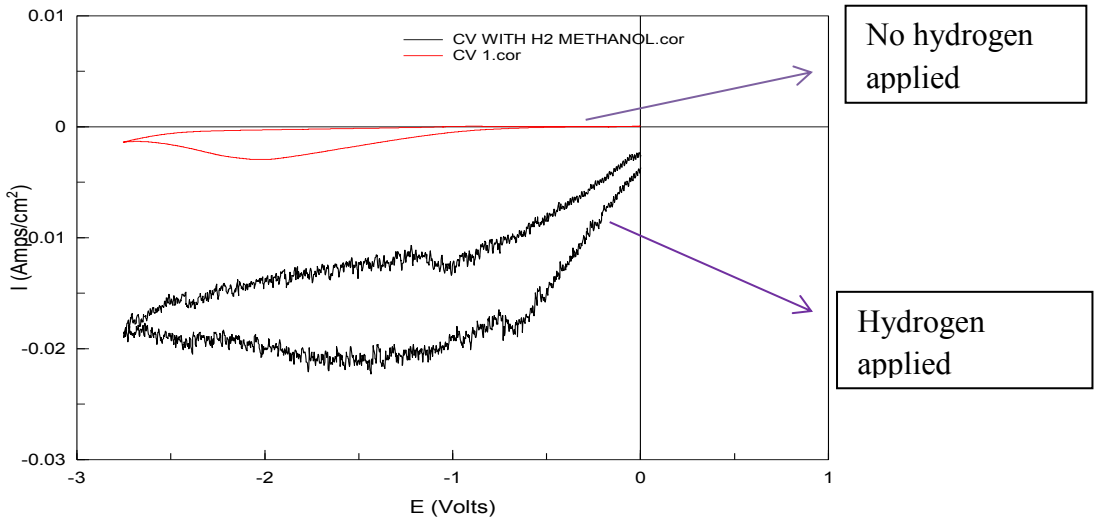


**Figure 54:** Overlay of cyclic voltammograms showing the effect $H_2$ application on current drawn.

These were positive results and so a potentiostatic experiment was set up to synthesize a substantial amount of the intended borohydride compound. The working electrode was set to -2.75 V and allowed to run for 10.5 h; at that point, the current was seen to be decreasing as shown in Figure 55.

Based on coulometric calculation, 0.147 M of the monoborohydride was synthesized in the cathode compartment.

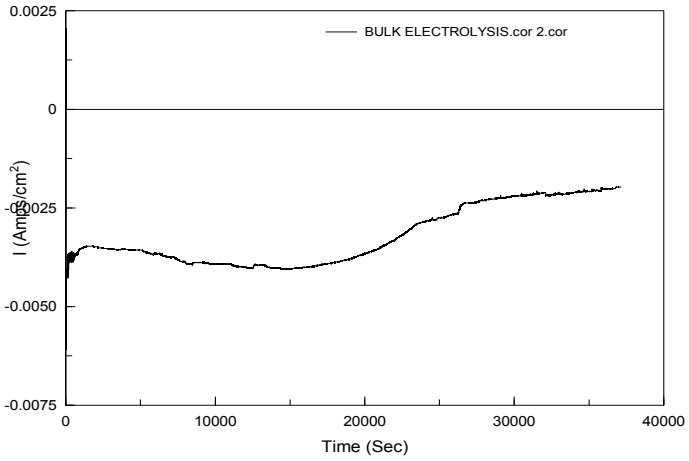


**Figure 55:** Potentiostatic current- time curve for borohydride synthesis in dual compartment cell. Electrode potential held at -2.75 V vs $Ag/AgClO_4$ for 10.5 h in 4.4 M TMB and 0.05 M $LiClO_4$ in $CH_3CN$. CE electrode compartment also contained 0.5 M methanol.

A portion of the electrolyte was collected and subjected to both IR and NMR spectroscopic analysis.

Figures 56 and 57 are IR spectra of the cathode compartment product at different scales.

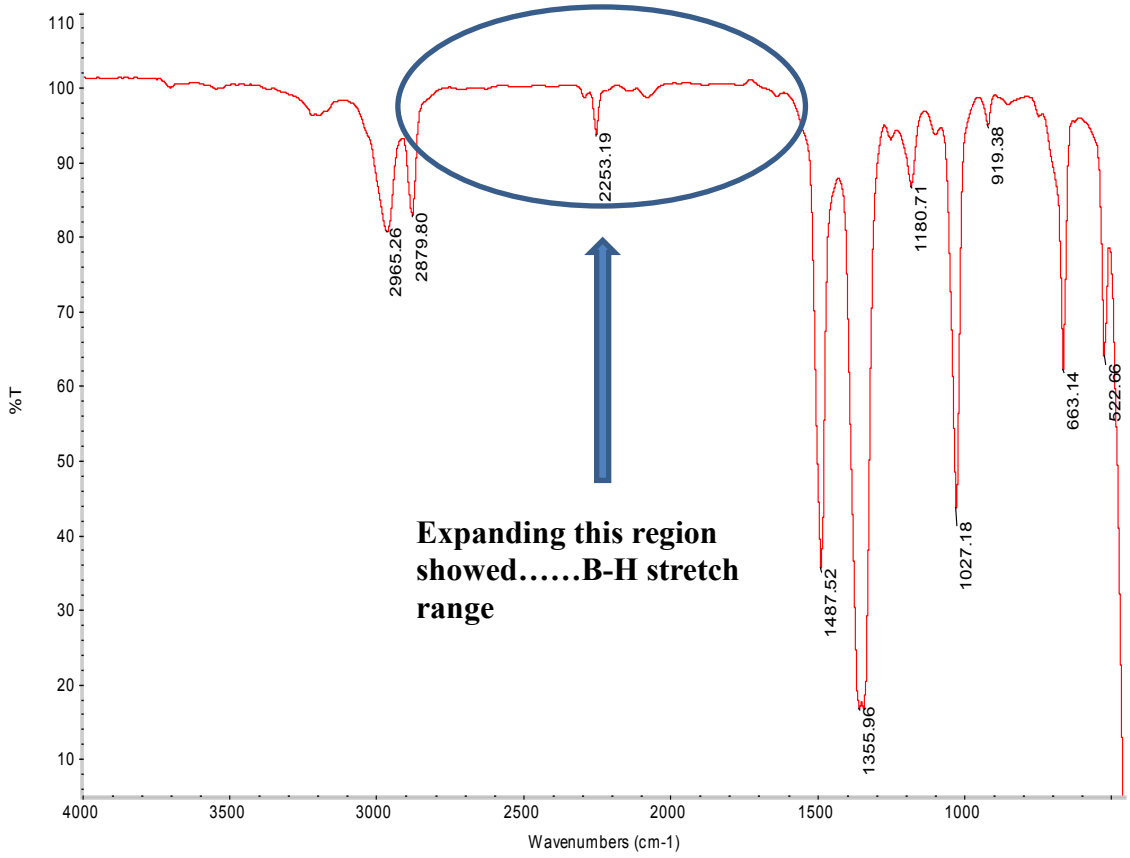


**Figure 56 :** IR spectrum of the cathode compartment contents containing 4.4 M TMB in 0.1 M $LiClO_4/CH_3CN$ after bulk electrolysis on Pd foil for 10.5 h at an applied voltage of -2.75 V.

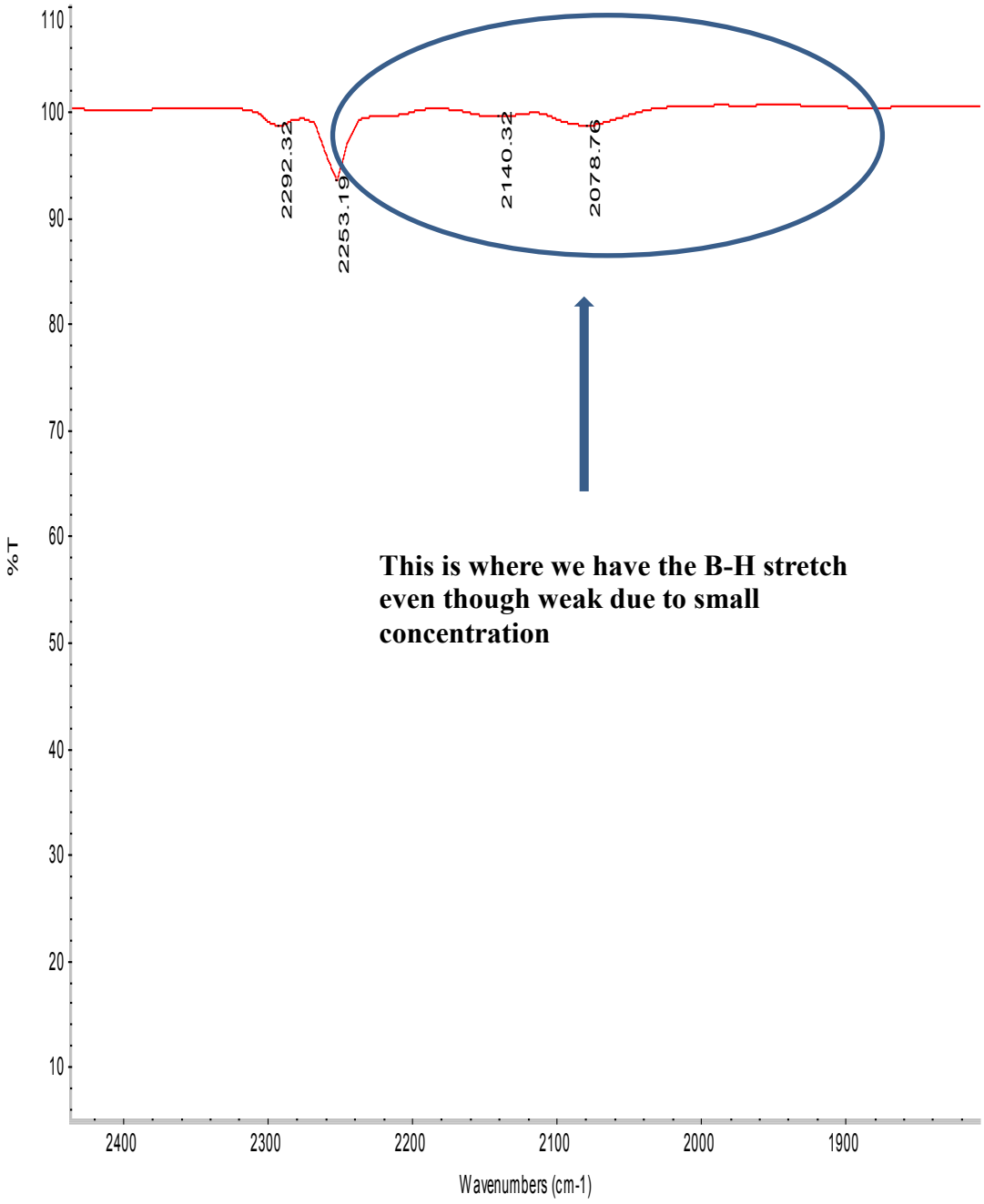


**Figure 57:** Expanded scale IR spectrum of the cathode compartment contents containing 4.4 M TMB in 0.05 M $LiClO_4/CH_3CN$ after bulk electrolysis for 10.5 h at an applied voltage of -2.75 V.

The IR literature values quoted in this thesis from reference 49 are in line with what was observed even though the absorption bands seem to be very weak.

The proton NMR spectrum of 0.5 M $LiBH_4$ dissolved in THF was taken in $CDCl_3$ to act as a reference spectrum. The spectrum obtained is shown in Figure 57.

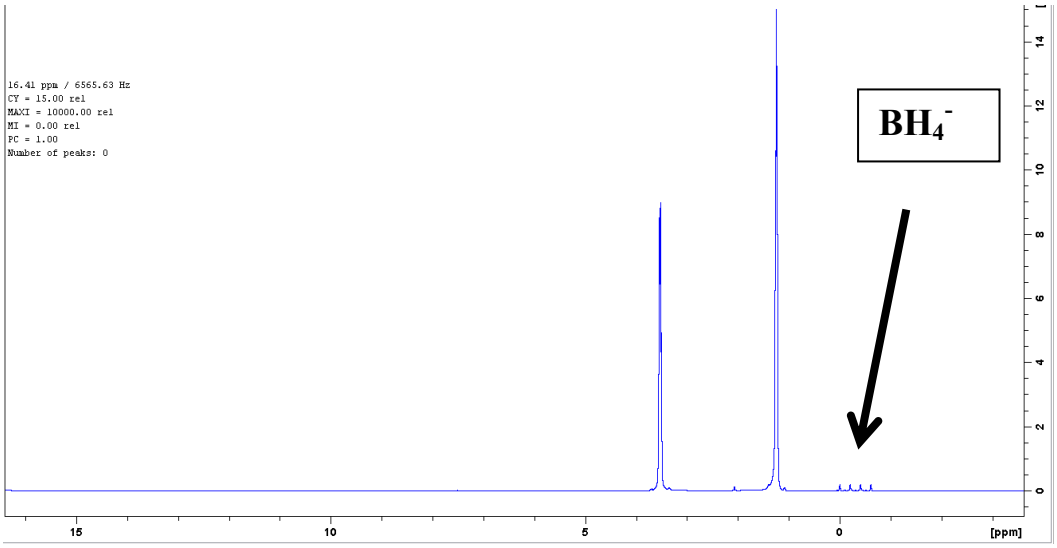


**Figure 58:** NMR spectrum of 0.5 M $LiBH_4$ dissolved in THF taken in $CDCl_3$ solvent.

The proton NMR in $CDCl_3$ of the product was done and the results obtained depicted in Figure 59 below.

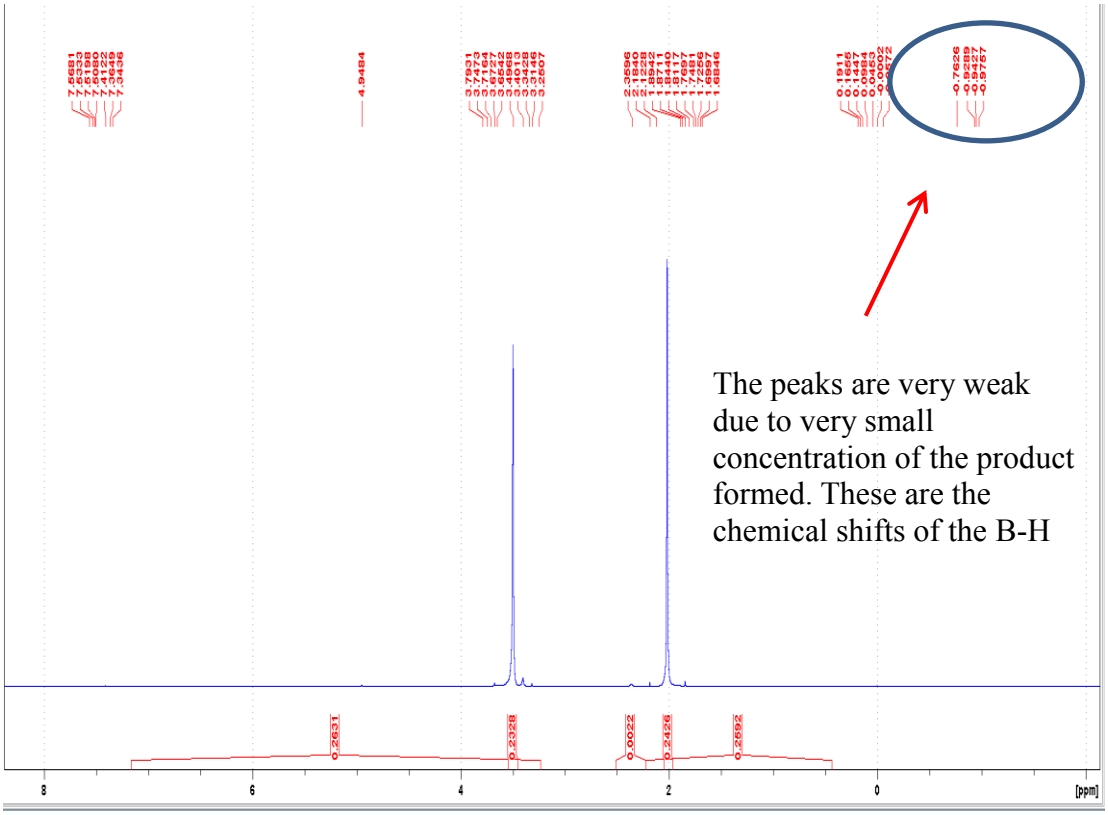


**Figure 59:** Proton NMR in $CDCl_3$ of the product of the cathode compartment after bulk electrolysis.

The NMR spectrum shows some negative chemical shifts to the left of the zero mark agreeing with the reference spectrum in Figure 57 of the borohydride ion. The weak nature of the peaks above is attributed to the low concentartion of the synthesized product.

## Chapter 4: Conclusion and future work

### Conclusion and future work.

This work has shown that the electrochemical combination of $H_2$ and TMB results in trace amounts of the borohydride as the electrolysis product. Electrochemical activity observed on Pd foil with TMB present underwent a tremendous increase in current whenever $H_2$ was applied from the back side of the cell. Products analyzed from the single compartment cell did not show enough evidence for the formation of the borohydride. Even though the Nafion membrane didn't completely separate the electrode reagents, analysis of the cathode compartment contents by IR confirms the formation of a B-H bond-containing compound in very low concentrations. The IR stretching bands of 2140.32 and 2078.76 $cm^{-1}$ from Figure 57 shows the presence of B-H bonds.

The proton NMR spectrum did not show significantly the formation of a B-H bond compound. However, on close examination, the spectrum shows some chemical shifts of -0.7, -0.92, -0.94 and -0.97 ppm. These chemical shifts conform to values for the chemical shifts of commercial B-H bond containing compounds like lithium borohydride shown in Figure 58. This serves as a confirmation that careful cell assembly and use of dry reagents and probably in situ analytical detection can give evidence on the formation of the borohydride through this electrosynthetic method.

THF was found to be an unsuitable solvent for this work since the supporting electrolyte remained undissociated in it. A more suitable solvent would be one in which lithium borohydride can dissolve and remain stable and electrochemically inert within the chosen potential window. Reasonable results were obtained in acetonitrile. Keeping away air and water, isolation of the product before analysis, stability of the cell to withstand $H_2$

pressure and frequent poisoning of the palladium foil remained important challenges in this work. Figuring out on how to carry out this experiment at elevated temperatures while keeping in mind the high flammability of $H_2$ will increase the yield. This is in line with various reports stating that hydride transfer occurs at elevated temperatures.

**References**


1. Ridley, S. Is our global warming and climate change 'truck' heading for the tipping point precipice?https://www.ice.org.uk/news-and-insight/the-civil-engineer/october **2018**/global-warming-truck-heading-for-precipice(accessed Dec 11, **2018**).
2. Nagpal, M.;Kakkar, R. An evolving solution: Intermediate hydrogen storage: *International Journal of Hydrogen Energy* , **2018**, 43, 12168-12188
3. Lim, K.L.; Kamezemian H.; Yakakob. Z.;Daud WRW. Solid-state materials and methods for hydrogen storage: a critical review. *Chemical Engineering Technology* ,**2010**, 33, 213-226.
4. B.D. Yacobucci, A.E. Curtright, CRS report for Congress, The Library of Congress, **2004**.
5. Schlapbach L, Zuttel A. Hydrogen-storage materials for mobile applications. *Nature* **2001**; 414:353-8.
6. Todorovic R. Hydrogen Storage Technologies for Transportation Application *Journal of Undergraduate Research* 2015; 5: 1
7. Thomas S. & Zalbowitz M. "Fuel cells green power," *Los Alamos New Mexico*.
8. Ozbilen A, Dincer I, Rosen M. A. "A comparative life cycle analysis of hydrogen production via thermochemical water splitting using a Cu-Cl cycle" *International Journal of Hydrogen Energy* **2011**; 36 , 11321-11327
9. Availablefrom:http://www2.dupont.com/FuelCells/en_US/products/literature.html
10. Prachi, R.P.; Mahesh, M.W.; Aneesh C.G.; A review on solid state hydrogen storage material. *Advances in Energy and Power* ,**2016**, 4 (2) 11-22

11. https://www.energy.gov/eere/fuelcells/hydrogen-storage
12. Züttel, A. Materials for hydrogen storage, *Materials Today*, 2003; 6, 24-33.
13. Ross, D.K. Hydrogen storage: the major technological barrier to the development of hydrogen fuel cell cars, *Vacuum* **2006**; 80. 1084-1089.
14. Vasiliev, L. L; Kanonchik,I. E; Kulakov,A. G; Mishkinis, D. A : "Activated carbon and hydrogen adsorption storage", Laboratory of Porous Media, *Luikov Heat & Mass Transfer Institute*, *National Academy of Sciences*, P. Brovka, 15, 220072, Minsk, Belarus
15. Dillon, A. C; Jones, K. M; Bekkedahl, T. A; Kiang, C. H ; Bethune, D. S; Heben, M. I. Storage of hydrogen in a single-walled carbon nanotube, *Nature*, **1997**; 386, 377- 379.
16. Tzimas; E., Filiou, S.D., Peteves and J.-B Veyret, "Hydrogen storage: State of the art and future perspectives", Petten, The Netherlands.
17. Victor Fernandes "Characterization of materials for hydrogen storage", *University of Manchester, Master's thesis*, **2010**.
18. Bououdina, M.; Grant, D., Walker, G. Review on hydrogen absorbing materials—structure, microstructure, and thermodynamic properties, *Int. J. Hydrogen Energy*, **2006**. 31, 177-182,
19. Sakintuna, B. Lamari-Darkrim, F. Hirscher, M. Metal hydride materials for solid hydrogen storage: A review, *Int. J. Hydrogen Energy*, **2007**; 32, 1121-1140,
20. Sandrock, G. & Thomas, G. The IEA/DOC/SNL on-line hydride databases. *Appl. Phys*. *A* **2001**; **72,** 153–155

21. Sakai, T., Natsuoka, M. & Iwakura, C. Rare earth intermetallic for metal–hydrogen

batteries. *Handb. Phys. Chem. Rare Earths,* **1995**. 21**,** 135–180

22. Kuriiwa T, Tamura T, Amemiya T, Fuda T, Kamegawa A, Takamura H. et al. New V-based alloys with high protium absorption and desorption capacity. *J Alloys Compds* **1999**; 433–6, 293–295:

23. Jain I P, Jain P, Jain A,. Novel hydrogen storage materials: A review of lightweight complex hydrides. *J. Alloys. Compd*., **2010**, Vol. 503, pp. 303-339

24. Bogdanovic´ B, Schwickardi M Ti-doped : alkali metal aluminium hydrides as potential novel reversible hydrogen storage materials. *J Alloy Compd* **1997**; 253–254:1–9

25. Chen P, Xiong Z, Luo J, Lin J and Tan L. *Nature***, 2002** ; 420, 302

26. Luo W. 2004. *J. Alloys Compd*. 381, 84

27. Manna J., Vashistha M., & Sharma P., "Lithium borohydride as Hydrogen storage material: A review," *International journal of energy for a clean Environment* 11 (1-4)

28. Wu Y., Kelly M.T., Ortega V.J., " Review of chemical processes for the synthesis of sodium borohydride, " **Millennium Cell Inc.** Under DOE Cooperative Agreement DE-FC36-04GO14008; **2004** August

29. Soulie´, J-Ph. Renaudin, Cerny´, G. R. Yvon* K. Lithium Boro-hydride $LiBH_4$ I. Crystal Structure, *Journal of Alloys and Compounds* , **2002**; 346 200–205.

30. Züttel A, Rentsch S, Fischer P, Wenger P, Sudan Mauron P, Emmenegger C Hydrogen storage properties of $LiBH_4$. *J Alloy Compd*, **2003**; 356–357:515–520.

31. Eberle U, Felderhoff M, Schüth F., " Chemical and physical solutions for hydrogen

Storage". *Angew Chem Int Ed* , **2009**; 48:6608–6630.

32. Walker G : Multicomponent hydrogen storage systems. In: Walker G (ed) Solid-state hydrogen storage: materials and chemistry. *Woodhead Publishing, Cambridge*, **2008.**

33. Schlesinger, H.I.; Brown, H.C. Metallo Borohydrides. III. Lithium Borohydride. *J. Am. Chem. Soc*., **1940**, 62, 3429–3435.

34. Puszkiel, J.; Garroni , S.; Milanese,C.; Gennari, F.; Klassen,T.; Martin Dornheim , M.; Pistidda, C. Tetrahydroborates: Development and potential as hydrogen storage medium. *Inorganics ,***2017**, 5,74 1-24

35. Schlesinger, H.I.; Brown, H.C.; Abraham, B.; Bond, A.C.; Davidson, N.; Finholt, A.E.; Gilbreath, J.R.; Hoekstra, H.; Horvitz, L.; Hyde, E.K., et al. New developments in the chemistry of diborane and the borohydrides. I. General Summary. *J. Am. Chem. Soc*., **1953**, 75, 186–190.

36. Friedrichs, O.; Borgschulte, A.; Kato, S.; Buchter, F.; Gremaud, R.; Remhof, A.; Züttel, A. Low-temperature synthesis of $LiBH_4$ by Gas– Solid Reaction. *Chem. Eur. J.*, **2009**, 15, 5531–5534

37. Schlesinger, H.I.; Brown, H.C.; Hyde, E.K. The preparation of other borohydrides by metathetical reactions utilizing the alkali metal borohydrides1. *J. Am. Chem. Soc*., **1953**, 75, 209–213.

38. https://www.asdlib.org/onlineArticles/ecourseware/Kelly_Potentiometry/PDF-17-Potentiostats.pdf

39. Sawyer T.D., Roberts J. L., JR. Experimental electrochemistry for chemists, *John Wiley and Sons New York.* **1974**.

40. Caroline R.Cloutier; Akram Alfantazi; Elod Gyenge physiochemical properties of alkaline aqueous sodium metaborate solutions, *J. Fuel Cell Sci*. *Technol,;***2006**; 4 (1) 88-98

41. Gyenge, E.L and Oloman, C.W, Journal of Applied Electrochemistry, **1998** 28 pp.1147-1151.

42. www.https://chem.libretexts.org/Bookshelves/Analytical_Chemistry/Book%3A_Analytical_Chemistry_2.0_(Harvey)/11_Electrochemical_Methods/11.4%3A_Voltammetric_Methods accessed july **17/2019**

43. Noemie Elgrishi,´ Kelley J. Rountree, Brian D. McCarthy, Eric S. Rountree, Thomas T. Eisenhart, and Jillian L. Dempsey A Practical Beginner's Guide to Cyclic Voltammetry *J. Chem. Educ*. **2018**, 95, 197−206

44. Zoski, C. G., Ed. Handbook of Electrochemistry; *Elsevier*: Amsterdam, The Netherlands, **2006**.

45. Bard, A. J.; Faulkner, L. R. Electrochemical Methods: Fundamental and Applications, 2nd ed.; John Wiley & Sons: Hoboken, NJ, **2001.**

46. Kounave P.S, Handbook of Instrumental Techniques for Analytical Chemistry, Tufts University, Department of Chemistry.

47. https://en.wikipedia.org/wiki/Nafion

48. Douglas A. Skoog, F. James Holler, Stanley R. Crouch Principles of *Instrumental Analysis 6$^{th}$ edition, Brooks/Cole*, Belmont *CA* 94002-3098, **2007**.

49. Biljana ˇSljuki´c,[*a] Diogo M. F. Santos,a Cesar A. C. Sequeira ´ [a] and Craig E. Banks[b] Analytical monitoring of sodium borohydride, *Anal. Methods*, **2013**, 5, 829, 2012.